Collective Excitations in Exotic Nuclei

David Radford (ORNL)
RIA Summer School, August 2002

I Nuclear Excitations: Single particle motion *vs*. Collective motion
Collective Modes: Rotations and Vibrations

II Experimental Techniques and Examples of Results
- Gamma-Ray Spectroscopy
  - High angular momentum
    - Band crossing and mixing
    - Band termination
    - Wobbling mode in triaxial SDBs
  - Towards the limits of stability
- Giant Resonances (high-frequency vibrations)
  - Photoabsorption
  - Hot, rotating nuclei
  - Pygmy resonance
  - Nuclear resonance fluorescence
- Intermediate-Energy Coulomb Excitation
  - Fragmentation beams, light (sd shell) nuclei

III Towards RIA: Experiments with n-rich beams at the HRIBF

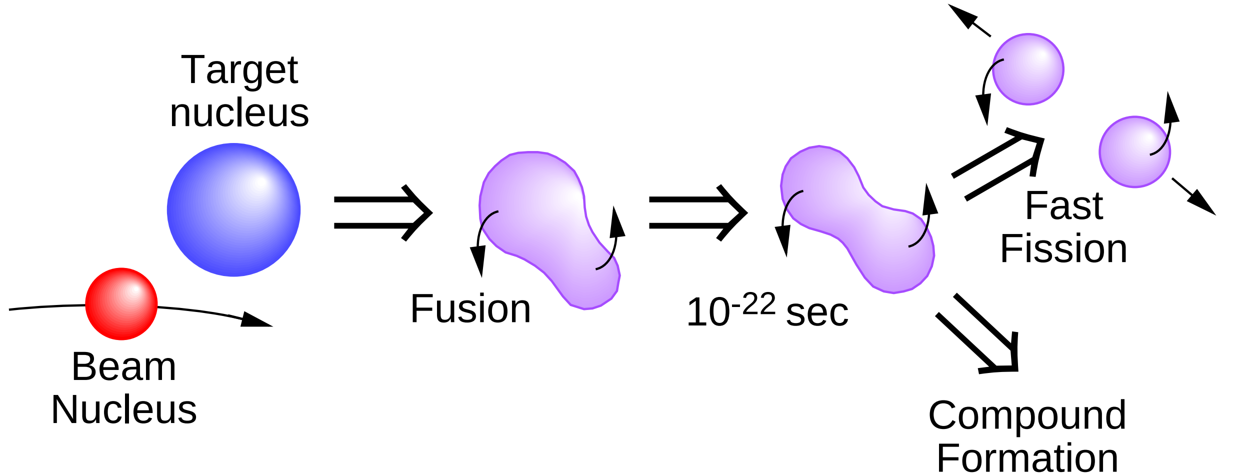

In-Beam Gamma Spectroscopy:

Fusion-Evaporation Reactions

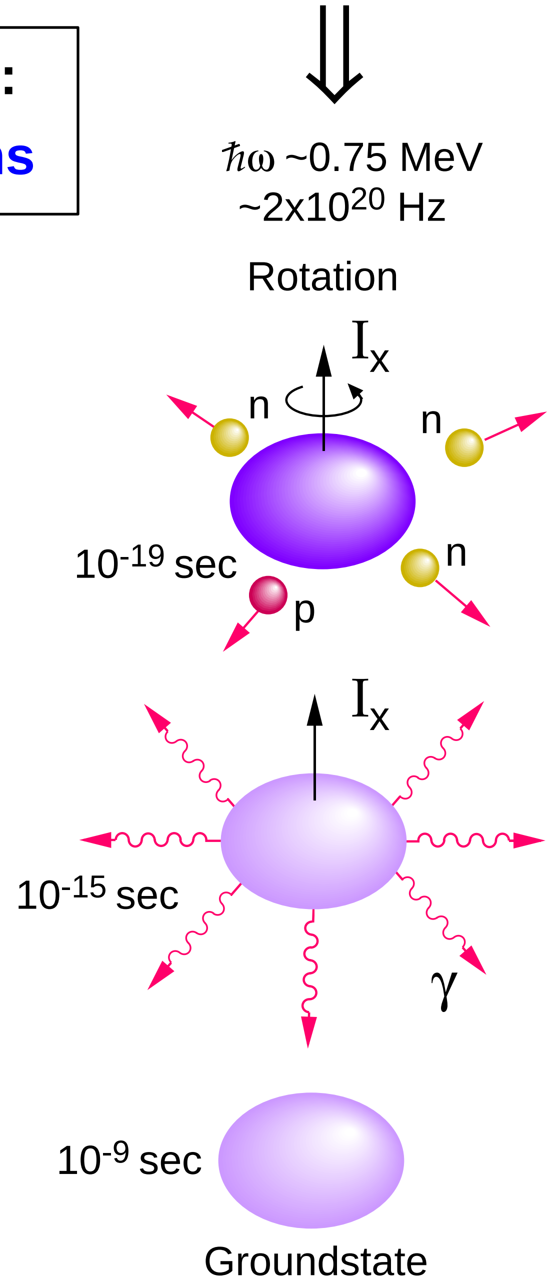

- Large cross section; ~1 barn
- Ideal for populating states with very high angular momentum (as high as ~70 ħ)
- Large gamma-ray multiplicity
  → need high-granularity high-efficiency high-resolution gamma detector array
- No Coulomb barrier for neutrons
  → tends towards proton-rich nuclei, hard to make neutron-rich

Gammasphere

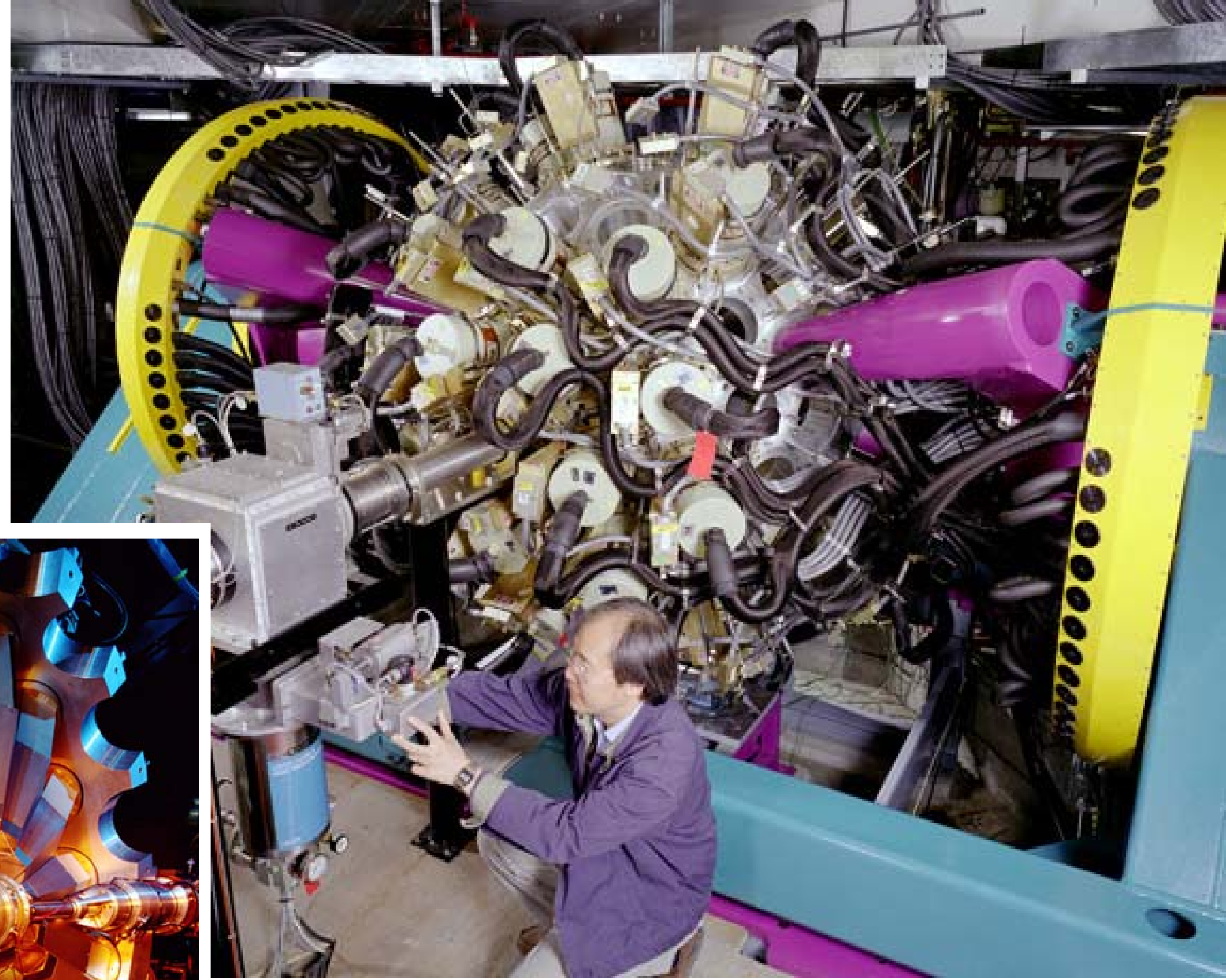

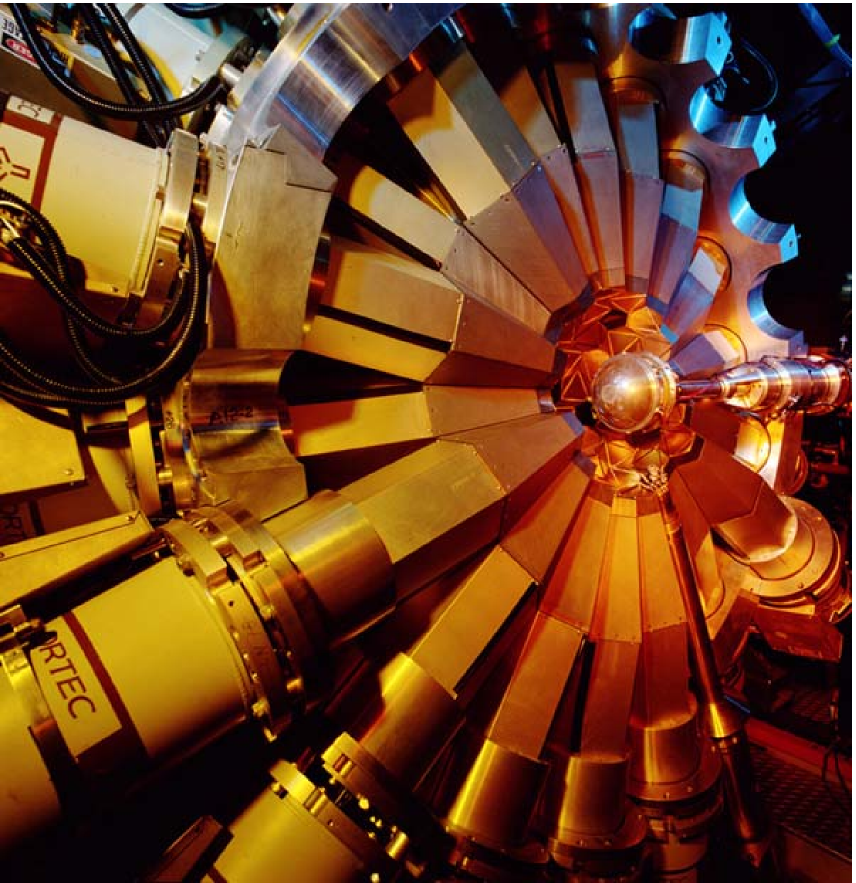

110 Compton-suppressed Ge detectors,
each with 70% efficiency.
Total efficiency = 9% at 1.3 MeV.

Euroball

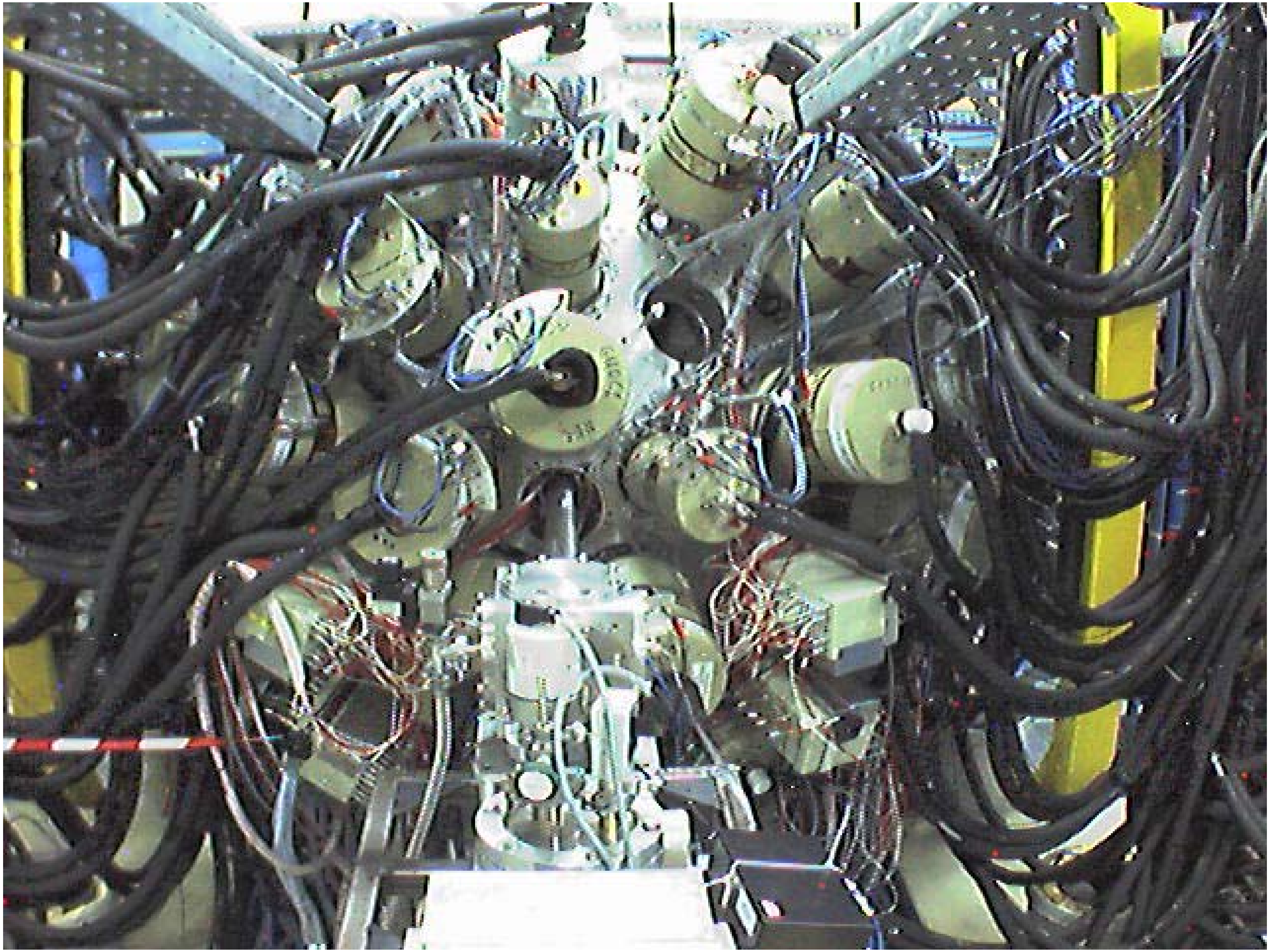

Improving Peak-to-Background - gated spectra

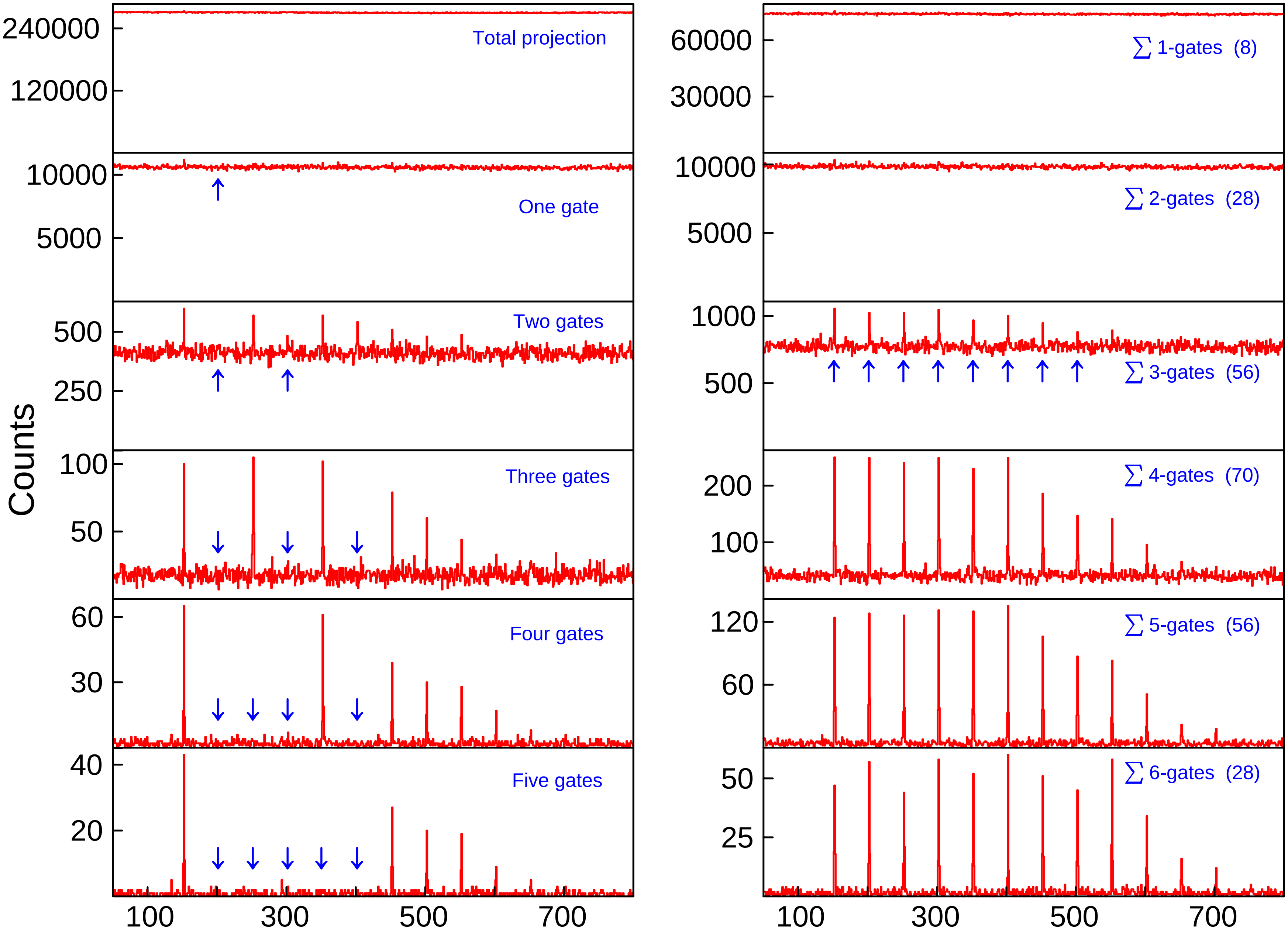

Sensitivity limit as a function of fold

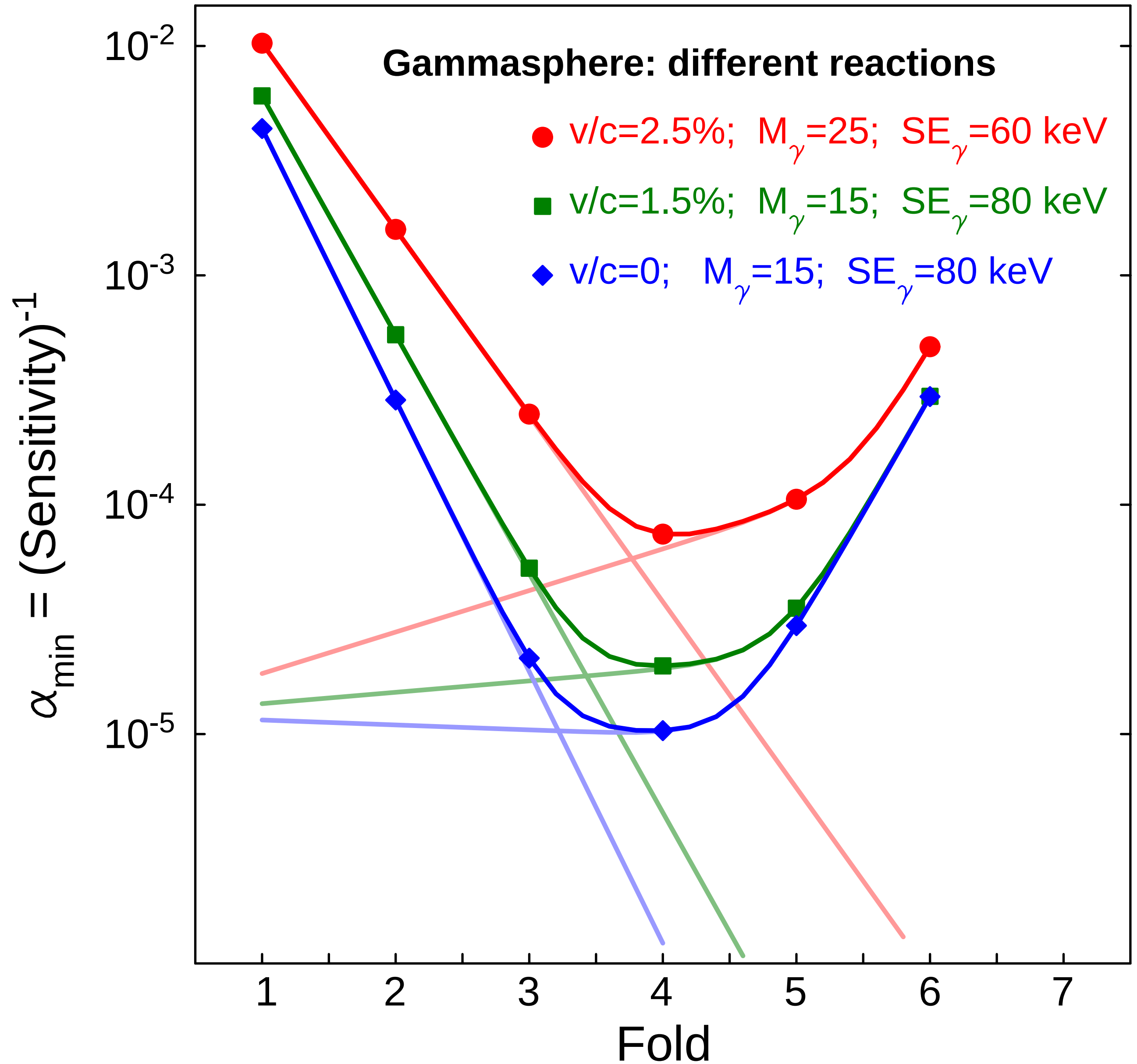

How close are we now to complete spectroscopy?

Selected examples of most-complete level schemes

- From RadWare level-scheme data base
- Sorted by number of gammas

Nuclide	Bands	Levels	Gammas	γ/level
^{174}Hf	34	347	516	1.49
^{163}Er	24	300	495	1.65
^{156}Dy	18	239	331	1.38
^{162}Tm	16	193	313	1.62
^{172}Hf	20	216	313	1.45
^{119}I	23	171	300	1.76
^{170}Lu	24	184	297	1.61
^{172}Ta	24	175	293	1.67
^{179}W	30	157	290	1.85
^{171}Lu	18	168	282	1.68
^{166}Hf	19	183	263	1.44

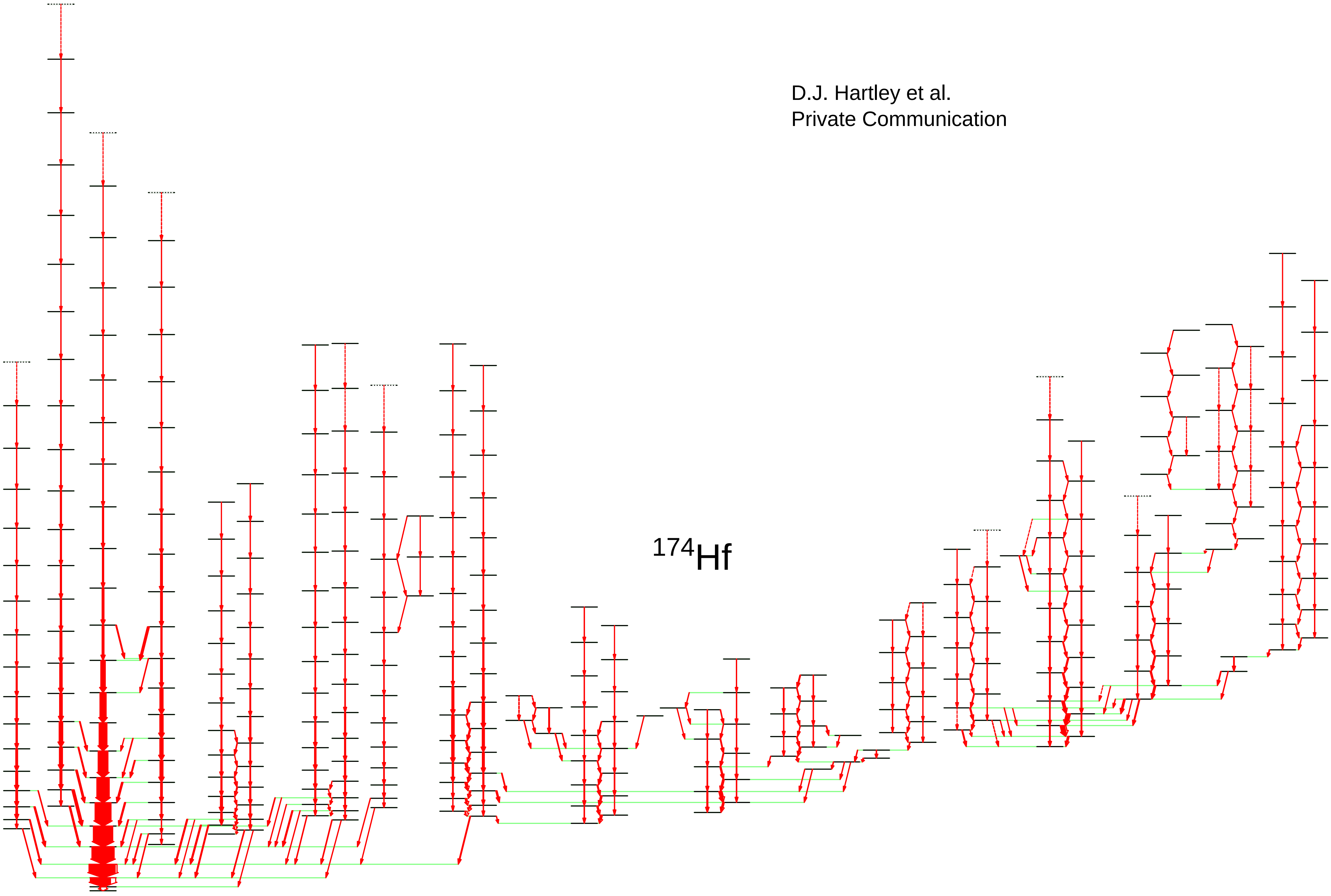
D.J. Hartley et al.
Private Communication
^{174}Hf

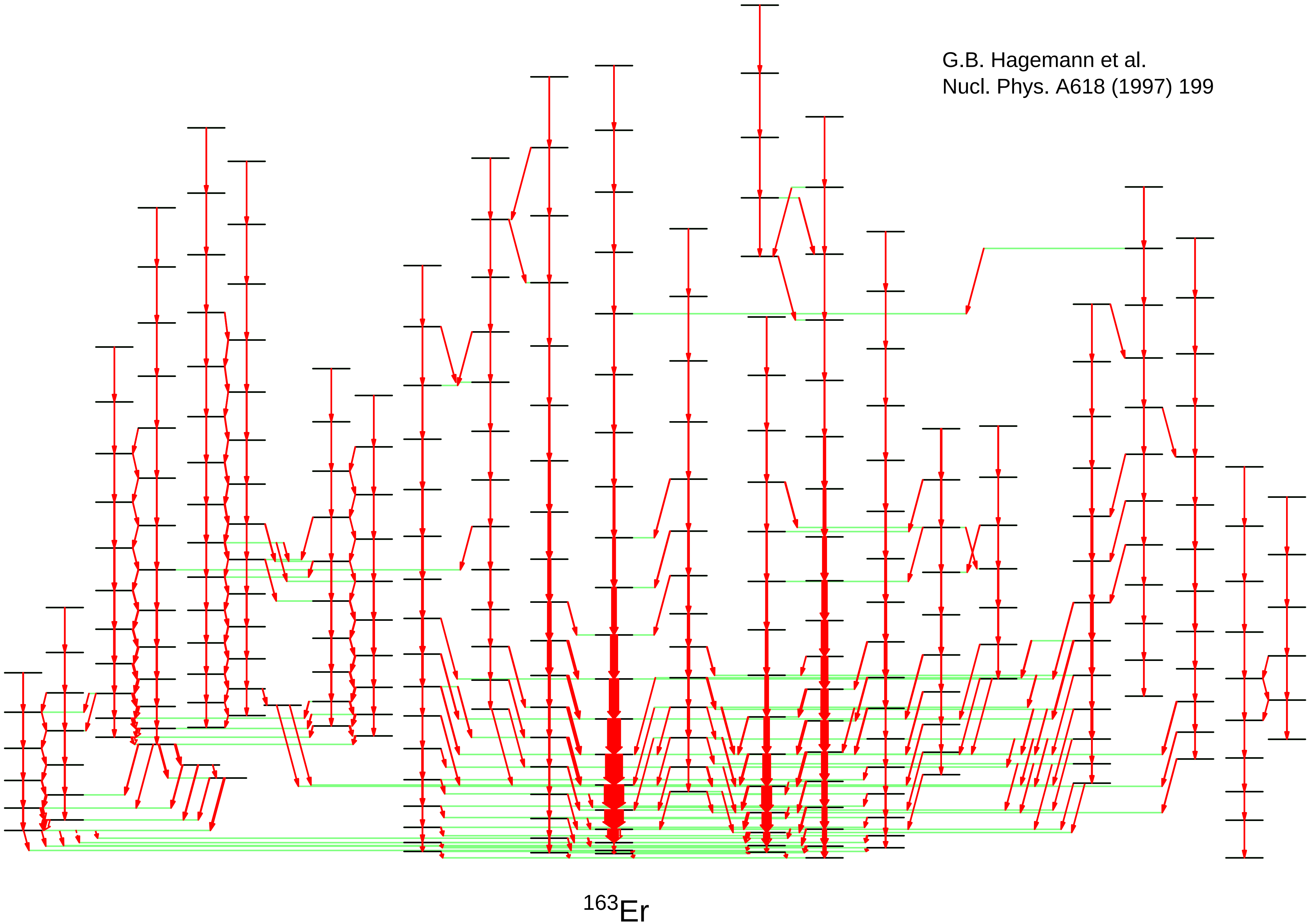
G.B. Hagemann et al.
Nucl. Phys. A618 (1997) 199
^{163}Er

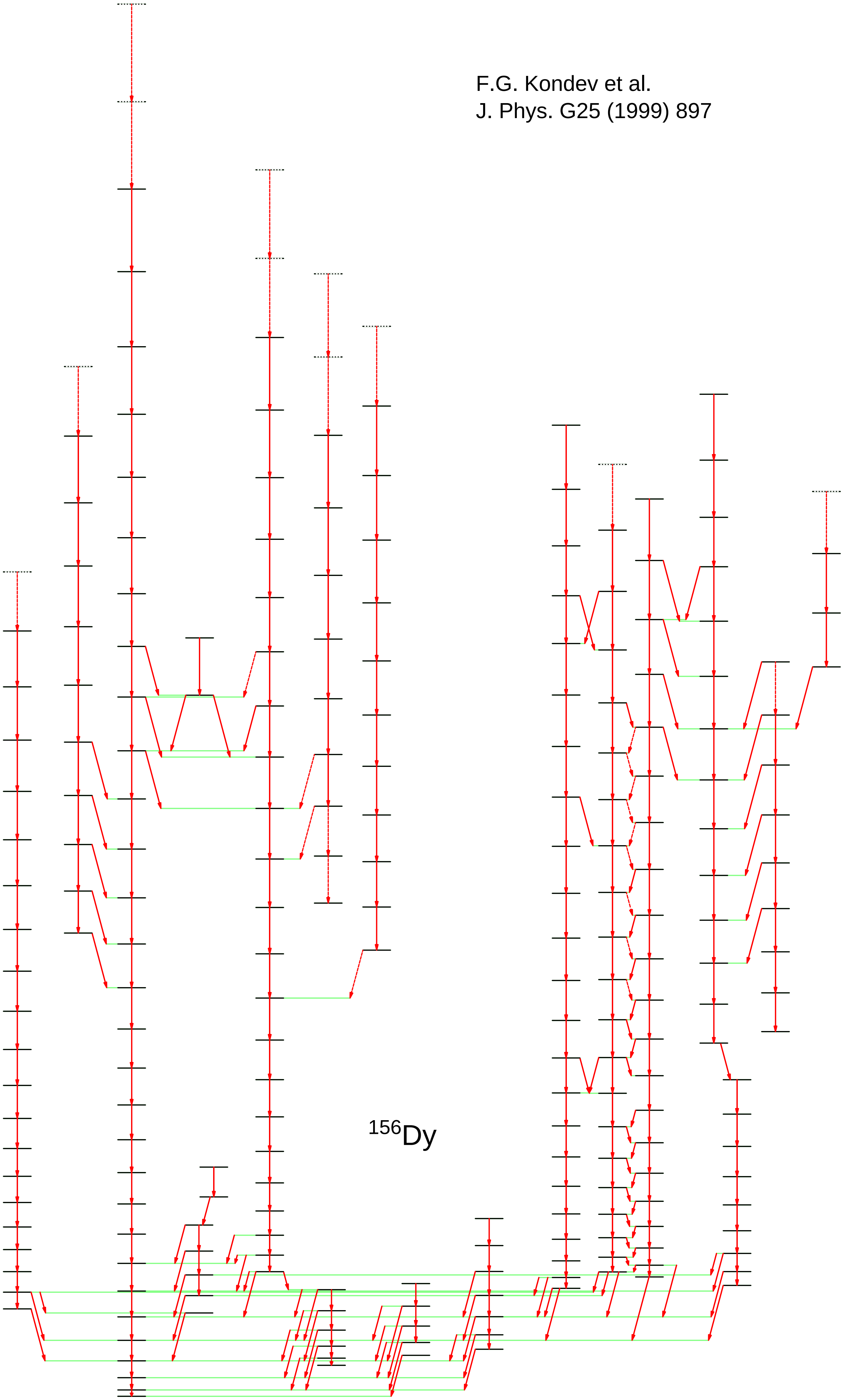
F.G. Kondev et al.
J. Phys. G25 (1999) 897
^{156}Dy

S. Erturk et al.
Private Communication

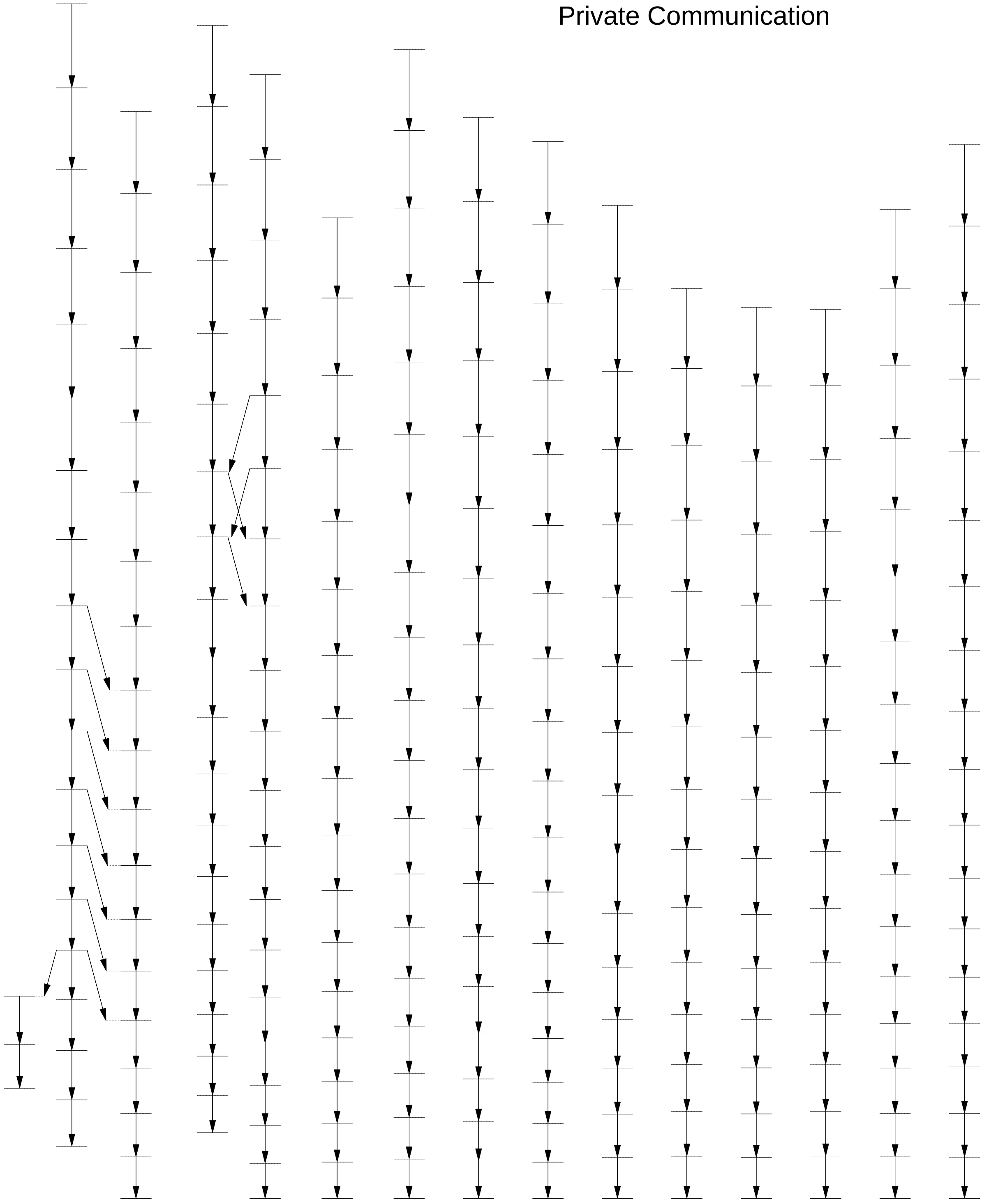

^{150}Gd Suderdef Bands

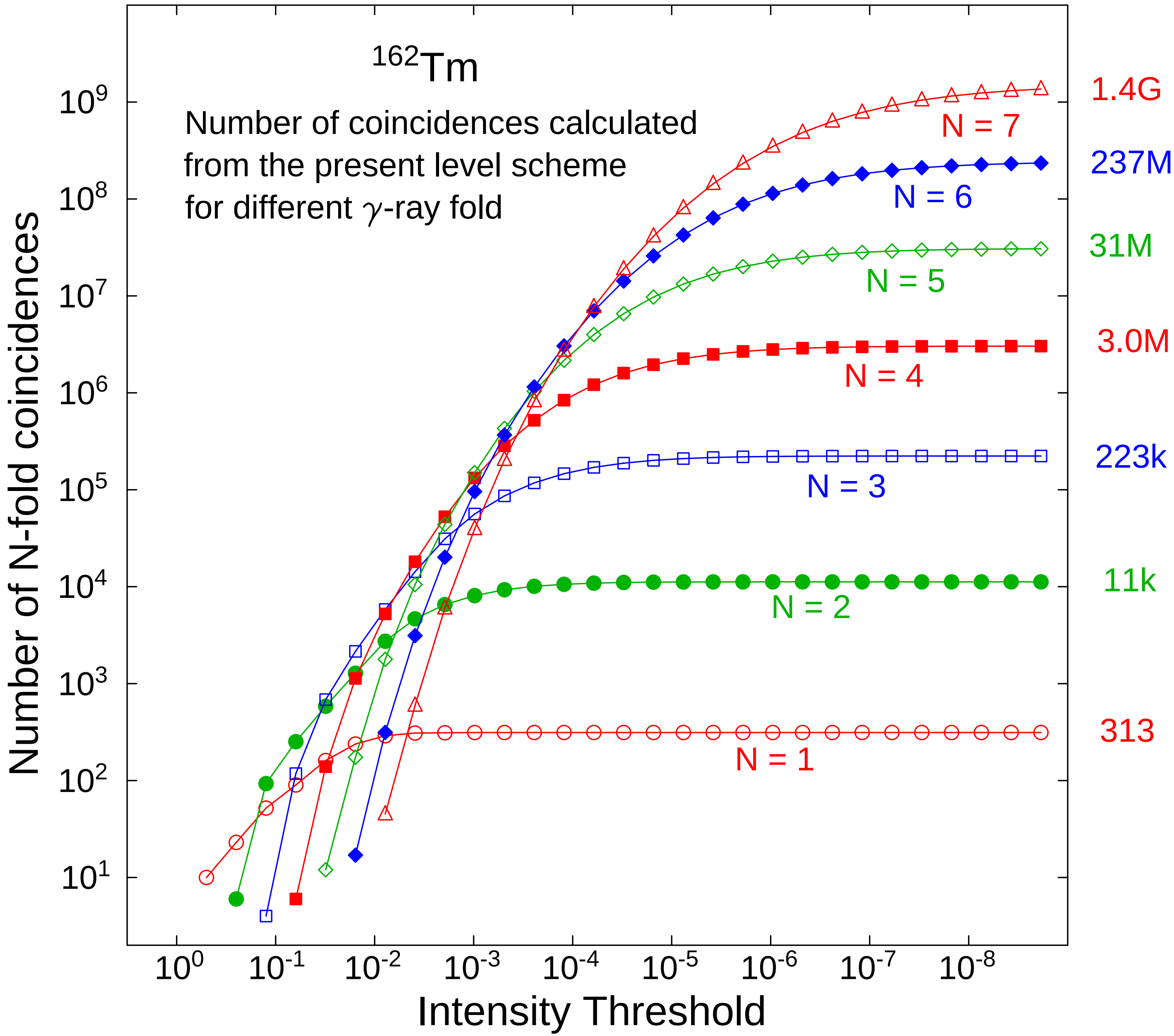

162Tm
Number of coincidences calculated
from the present level scheme
for different γ-ray fold
Number of N-fold coincidences
Intensity Threshold
N = 7
N = 6
N = 5
N = 4
N = 3
N = 2
N = 1
1.4G
237M
31M
3.0M
223k
11k
313
10^9
10^8
10^7
10^6
10^5
10^4
10^3
10^2
10^1
10^0
10^-1
10^-2
10^-3
10^-4
10^-5
10^-6
10^-7
10^-8

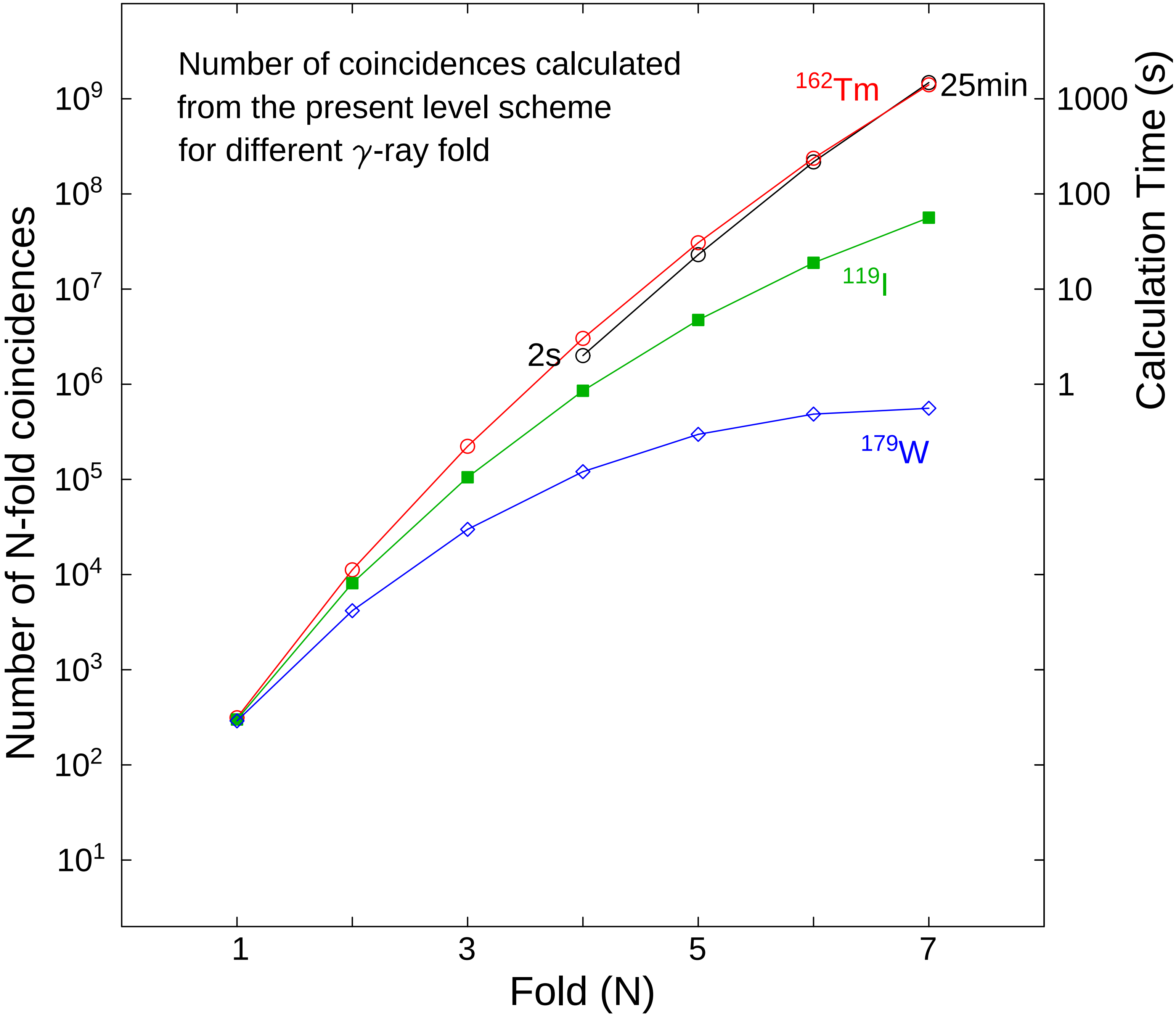

Number of coincidences calculated
from the present level scheme
for different γ-ray fold
^{162}Tm
25min
2s
^{119}I
^{179}W
10^9
10^8
10^7
10^6
10^5
10^4
10^3
10^2
10^1
Number of N-fold coincidences
1000
100
10
1
Calculation Time (s)
1
3
5
7
Fold (N)

G.B. Hagemann et al., Nucl. Phys. A618 (1997) 199

(a)

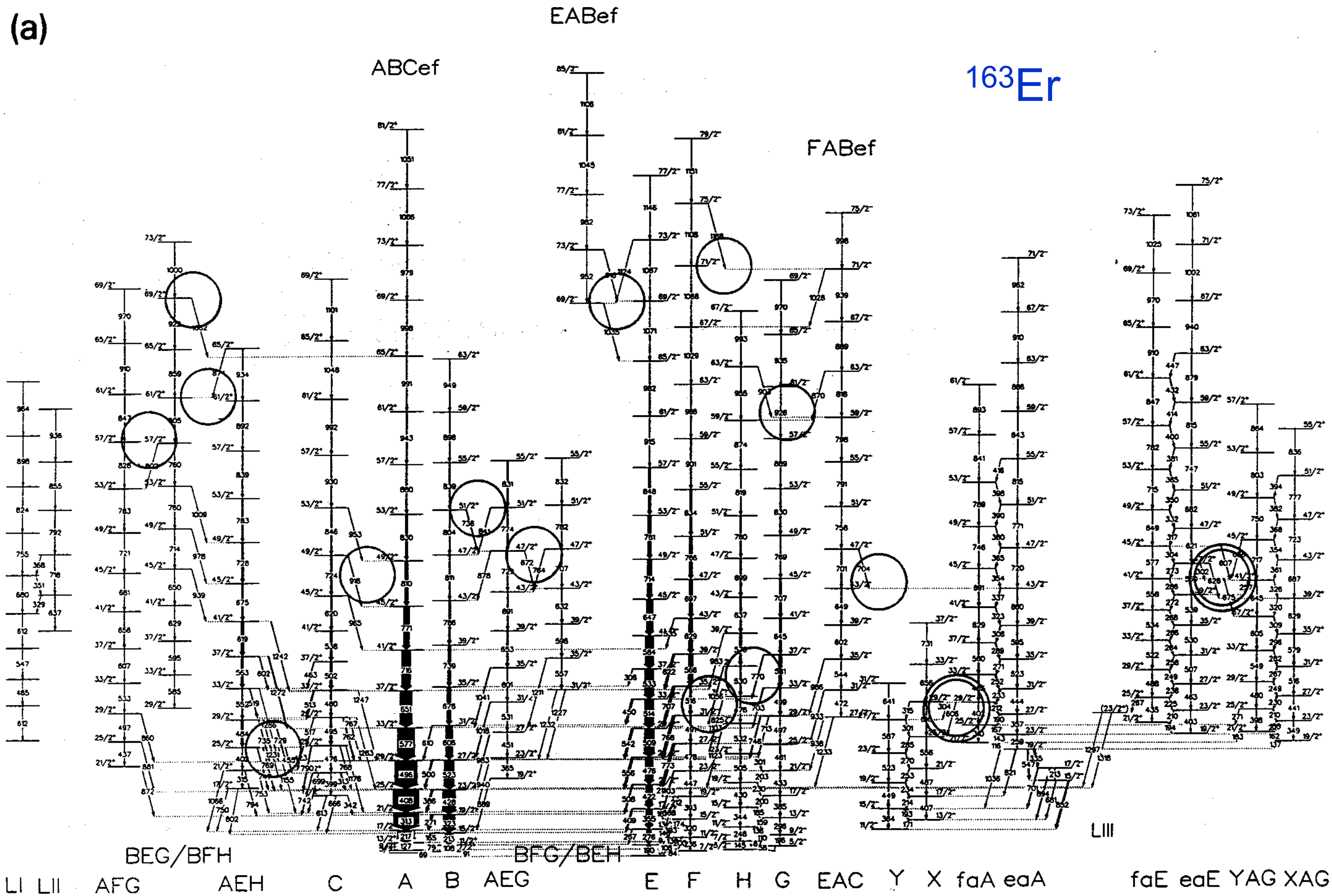

Fig. 1. (a) The full level scheme of ^{163}Er. Circles mark crossings of bands where E2 cross-band transitions are observed.

^{163}Er

Fig. 3. Excitation energies for rotational bands in ^{163}Er as a function of spin. A reference $AI(I+1)$ has been subtracted with $A = 8.7$ keV. The upper quadrangles show bands with negative parity and signatures $+1/2$ and $-1/2$, while the lower quadrangles show bands with positive parity and signatures $+1/2$ and $-1/2$.

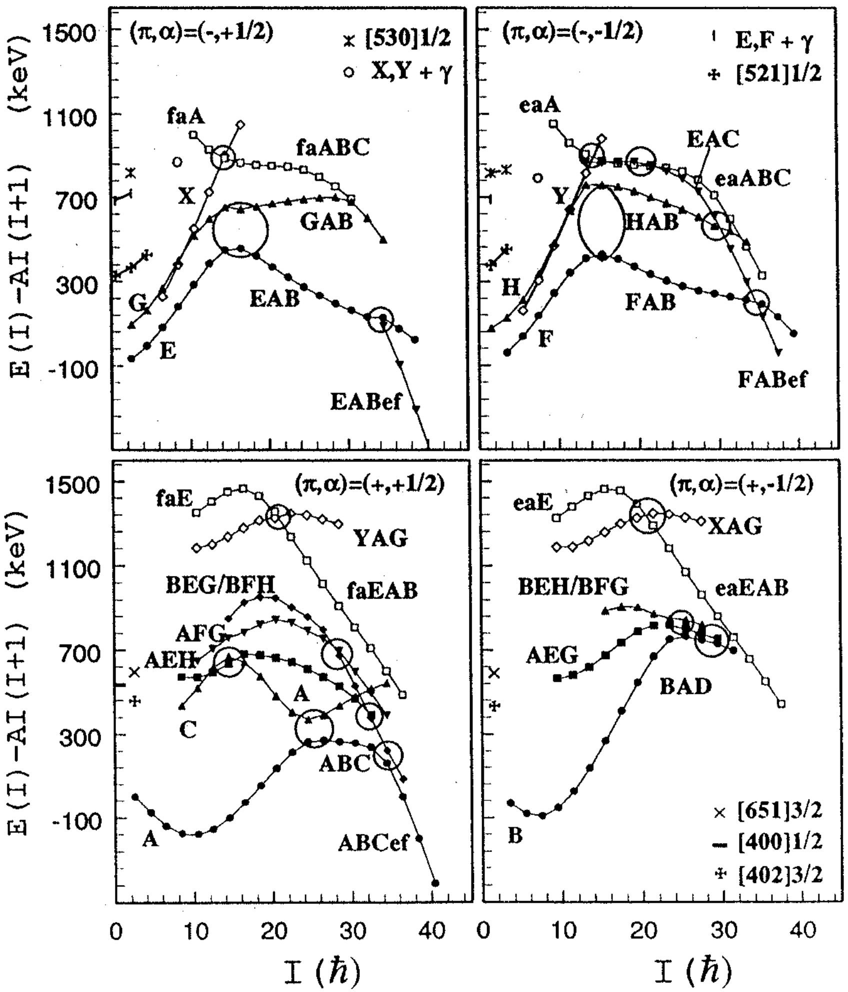

G.B. Hagemann et al., Nucl. Phys. A618 (1997) 199

Circles show band crossings where E2 cross-band transitions are observed. These are used to accurately determine the inter-band interaction strength.

Table 4

Interactions between rotational bands in ^{163}Er. Cases where both bands are known below and above the crossing are included. For the classification of assignments see Table 3. Orbitals changed in the interaction are underlined

K_1	Interacting bands Label$_1$⟺Label$_2$	K_2	Strength V [keV]	~ΔK [$\hbar$]	~Spin [$\hbar$]	~Δi [$\hbar$]
11/2	X⟺G[a]	3/2	< 2	4	11	0
11/2	Y⟺H[a]	3/2	< 2	4	11	0
5/2	EAB⟺GAB	3/2	50–80	1	16	0
5/2	FAB⟺HAB	3/2	< 150	1	16	0
7/2[b]	C(γ)⟺AEH	9/2[b]	< 11	1	13	0
5/2	A⟺ABC	5/2	49	0	24	4
5/2	ABC⟺ABCef	5/2	25–30	0	35	5.5
5/2	EAB⟺EABef	5/2	~15	0	34	5
5/2	FAB⟺FABef	5/2	~15	0	34	4.5
5/2	BAD⟺AEGBC	9/2[b]	(~13)	2	29	0
9/2[b]	BEHAD⟺AEGBC	9/2[b]	(~14)	0	23	0
9/2[b]	AEHBC⟺ABCef	5/2	~6	2	32	5
9/2[b]	AFGBC⟺ABCef	5/2	~11	2	28	4
3/2	HAB⟺FABef	5/2	~10	1	29	4
13/2[b]	EAC⟺eaA	19/2	1–2	3	21	0
11/2	X⟺faA	19/2	1.4	3	15	3.5
11/2	Y⟺eaA	19/2	1.3	3	15	3.5
19/2	XAG⟺eaEAB	19/2	16	0	21	3.5
19/2	YAG⟺faEAB	19/2	14	0	21	3.5

Smooth Band Termination

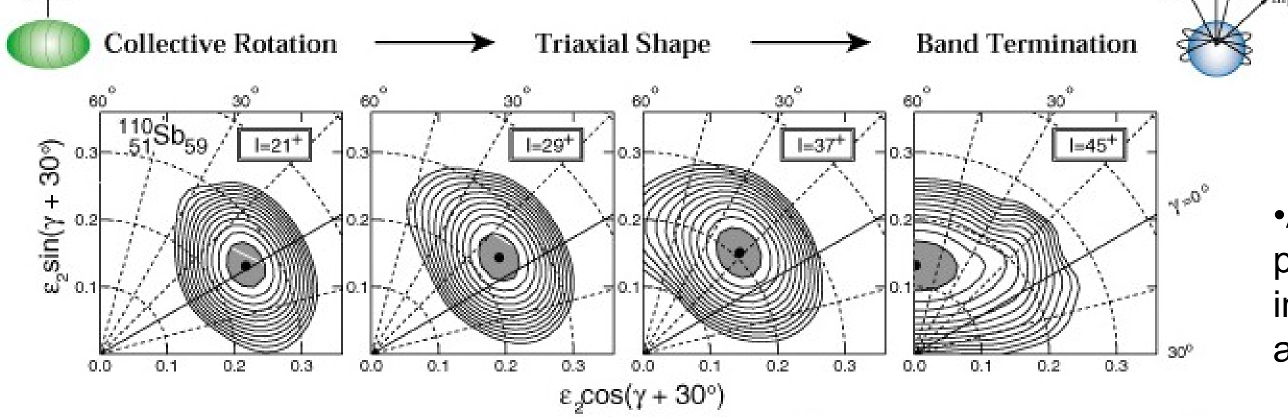

^{110}Sb yrast band configuration information $[21, 3] \equiv \left[\#\pi g_{9/2}^{-1}\ \#\pi h_{11/2},\ \#\nu h_{11/2}\right]$

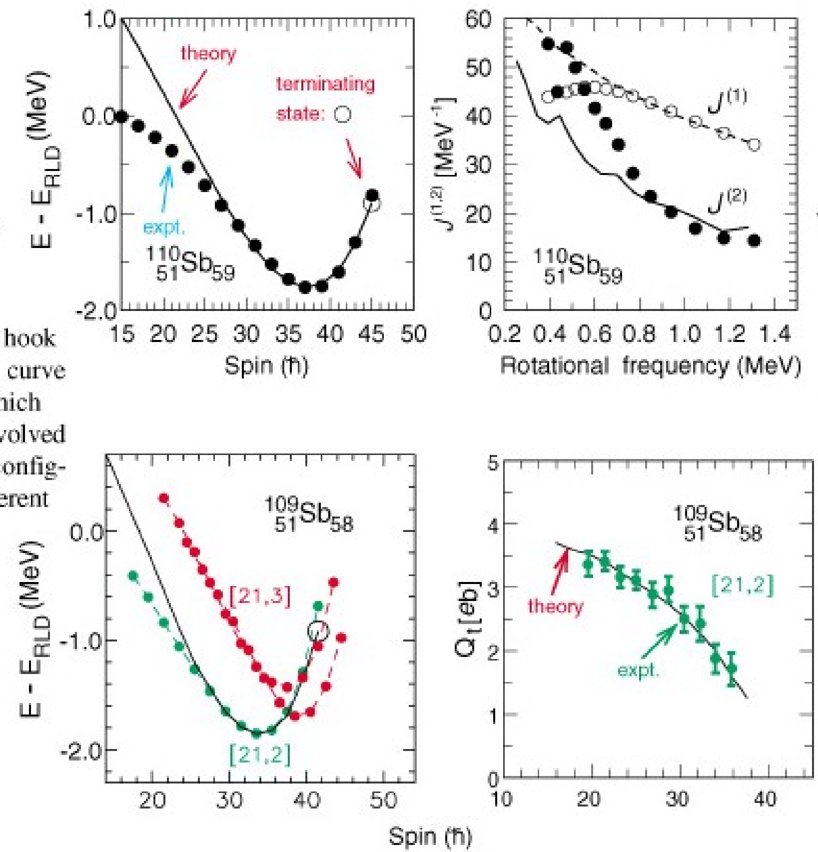

Characteristic hook shape E-E$_{RLD}$ curve depends on which orbitals are involved in each band configuration in different nuclei.

Kinematic and Dynamic moments of inertia $J^{(1)}$, $J^{(2)}$ **and** quadrupole moment Q_t decrease with increasing spin as the gradual change from prolate to oblate shape occurs.

- At medium spin, the nucleus is a prolate collective rotor. As spin is increased, it changes smoothly to an oblate non-collective shape.
- The nucleus changes the mechanism by which it generates angular momentum, from collective rotation perpendicular to the symmetry axis, to single-particle alignment.
- The rotational band terminates at an angular momentum that exhausts the total aligned spin of the valence particles.

Wobbling Mode of Triaxial Superdeformed Nuclei

S.W. Ødegård et al.,
Phys. Rev. Lett. 86 (2001) 5866

Cranking:

Wobbling:

-Requires Triaxialty!

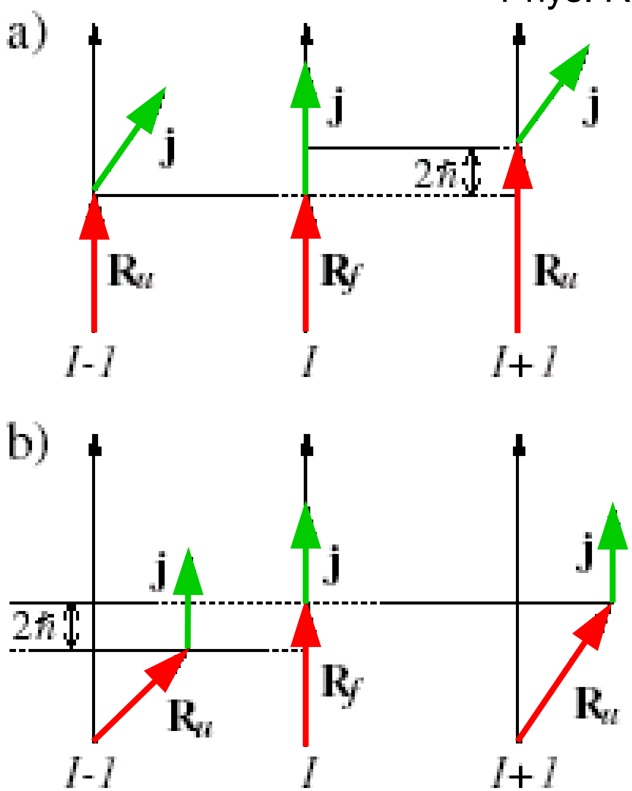

FIG. 4. Schematic coupling scheme of the particle and core angular momenta in the favored (I) and unfavored ($I \pm 1$) states for (a) the cranking regime and (b) the wobbling mode ($n_w = 1$). The total angular momentum is $\mathbf{I} = \mathbf{R} + \mathbf{j}$, where the angular momentum of the collective rotation of the core is expressed by $\mathbf{R}$. The vertical axis shown (x axis) is the axis of the largest moment of inertia of the core, about which collective rotation is energetically cheapest. For $n_w > 1$ the angle between the x axis and $\mathbf{R}$ gets larger.

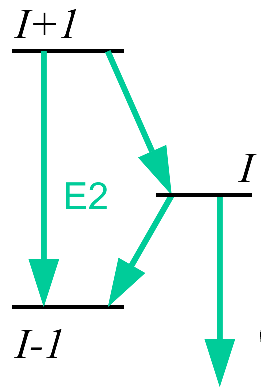

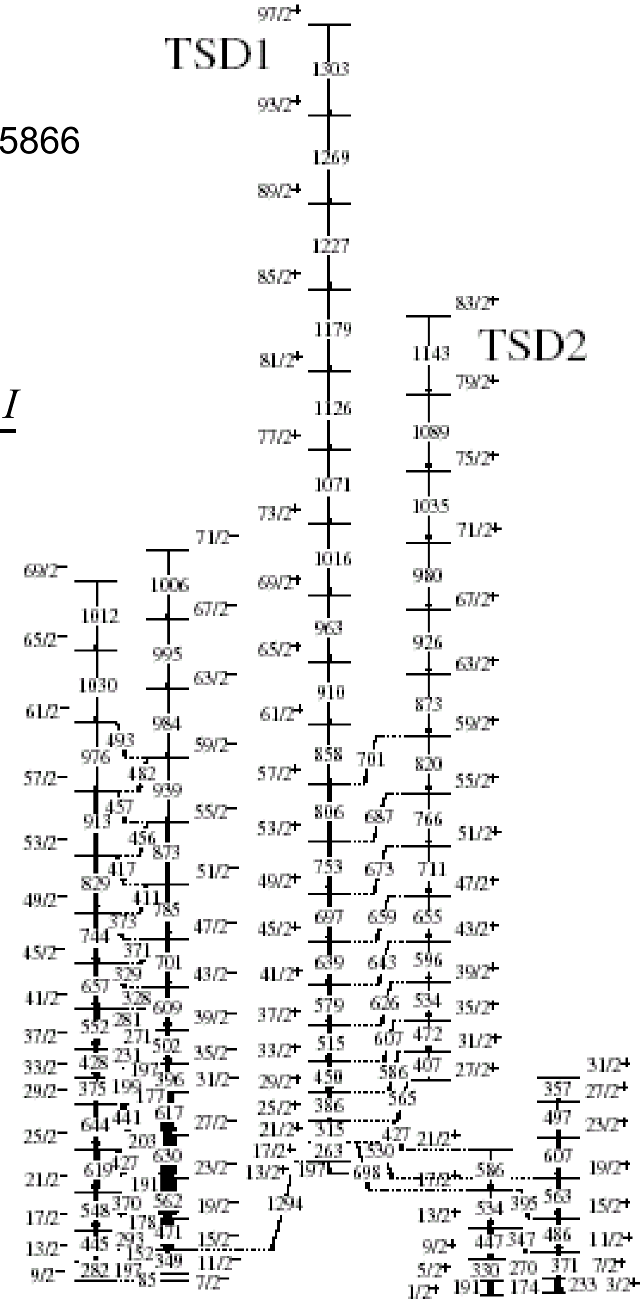

FIG. 1. Partial level scheme of ^{163}Lu showing the two TSD bands together with the connecting transitions and the ND structures to which the TSD states decay.

RECOIL DECAY TAGGING METHOD

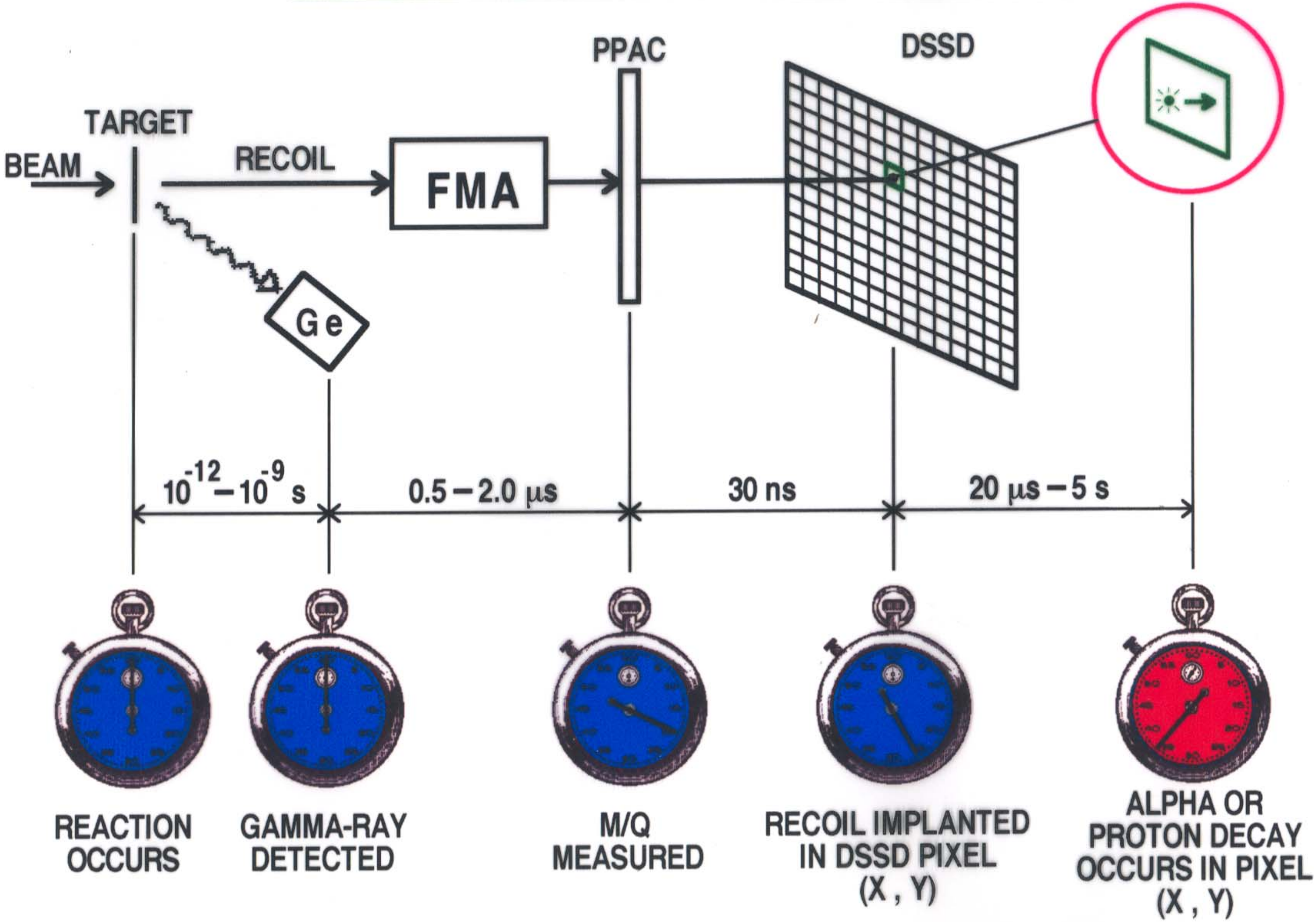

1. Prompt γ-rays correlated with M/Q and (X , Y) position of recoil in DSSD
2. Decay proton or alpha identifies nucleus that emitted the γ-rays

Example of Recoil-Decay Tagging: ^{109}I

C.-H. Yu et al., Phys. Rev. C59 (1999) R1836

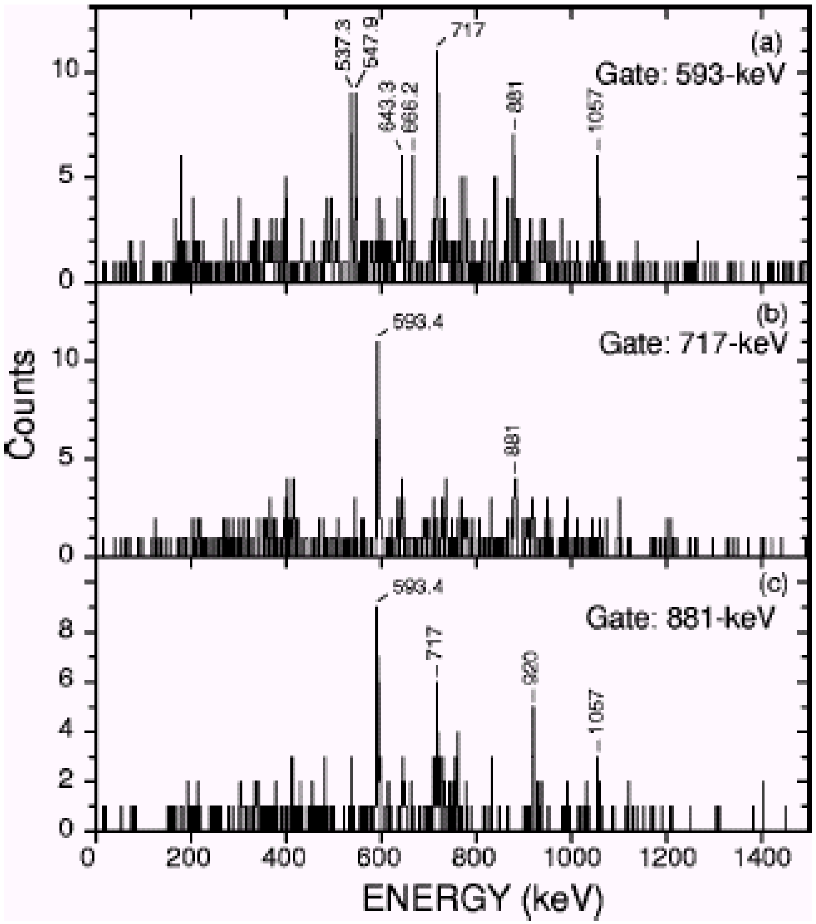

FIG. 2. Gamma-ray spectra obtained by gating on the (a) 593-keV, (b) 717-keV, and (c) 881-keV transitions in the $\gamma\gamma$ coincidence matrix that is correlated with the 829-keV ground-state proton decay in ^{109}I.

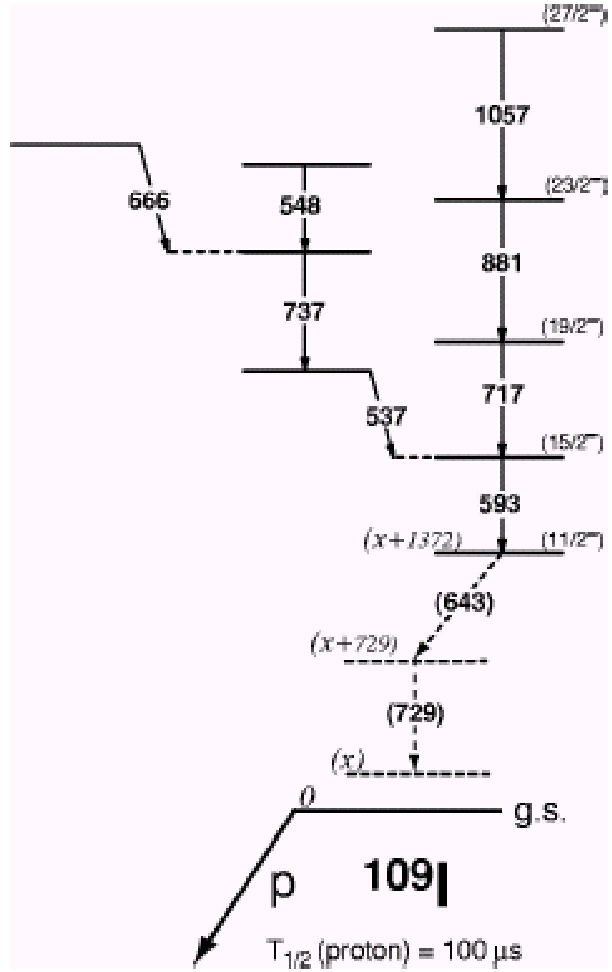

FIG. 3. Proposed level scheme of ^{109}I based on the present work. See text for detailed arguments for the placement of transitions and their spin and parity assignment.

Gamma Spectroscopy of ^{254}No

P. Reiter et al.,
Phys. Rev. Lett. 84 (2000) 3542

- Observe discrete transitions to spin 20
- Measured entry distribution in (E_X, I)
- Provides new data on formation mechanism and fission barrier.

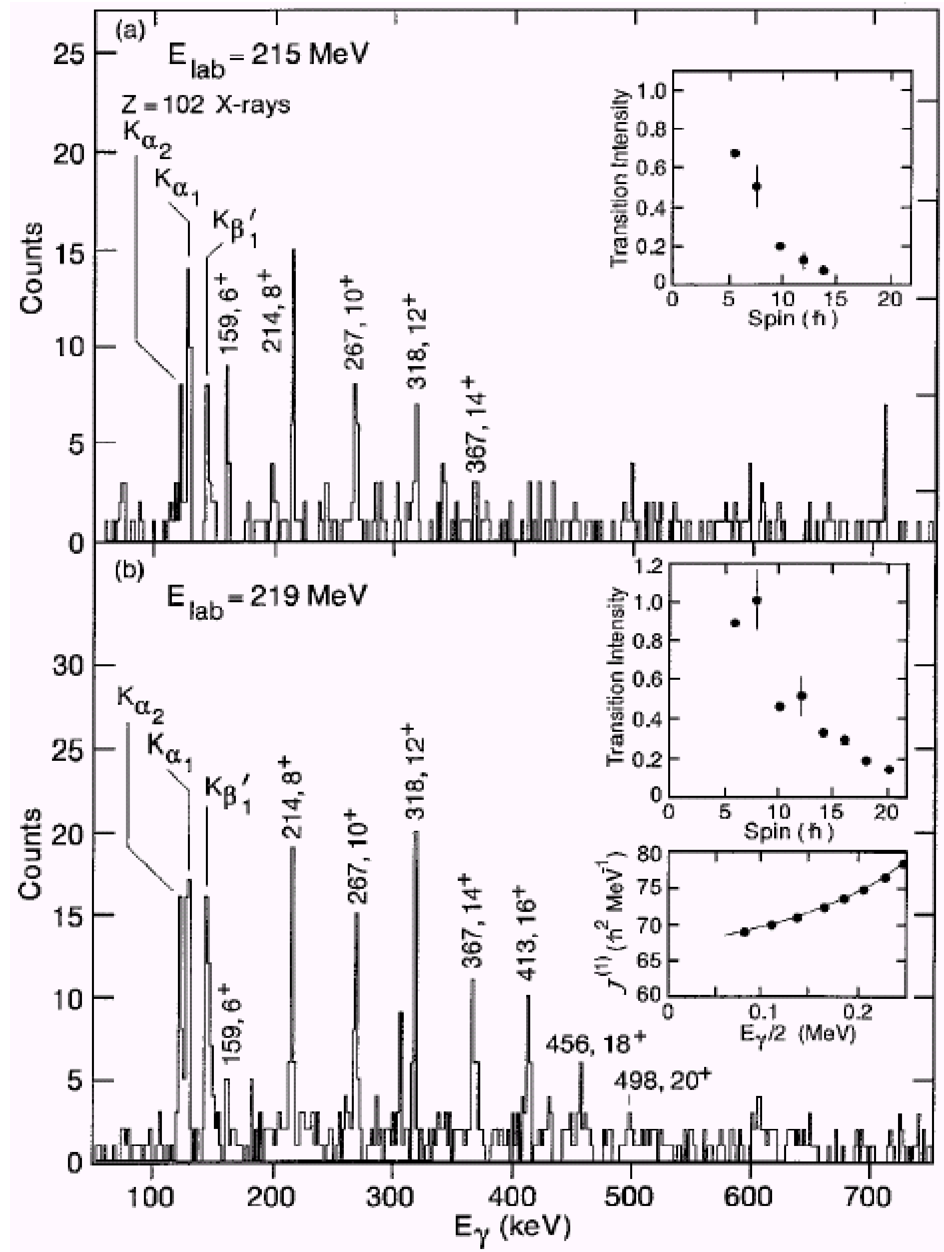

FIG. 1. ^{254}No γ spectra, obtained by requiring recoil-γ coincidences in Gammasphere and the FMA focal-plane detectors,

The Giant Dipole Resonance

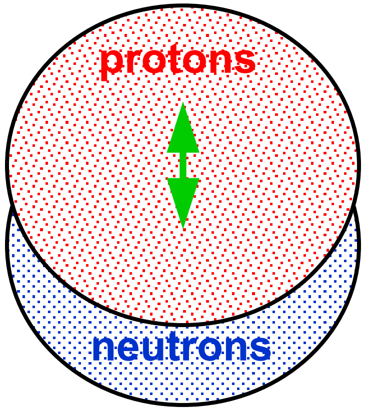

The GDR can be considered as an oscillation of the protons against the neutrons. This results in a large oscillating electric dipole moment.

Since the protons and neutrons are moving differently, the isospin T = 1; this is the Isovector GDR.

$$\frac{E}{\Gamma} \sim \frac{14\ \text{MeV}}{4.2\ \text{MeV}} \sim 3.5$$

→ Strongly damped.

S. Kamerdzhiev and J. Speth, Nucl. Phys. A599 (1996) 373c

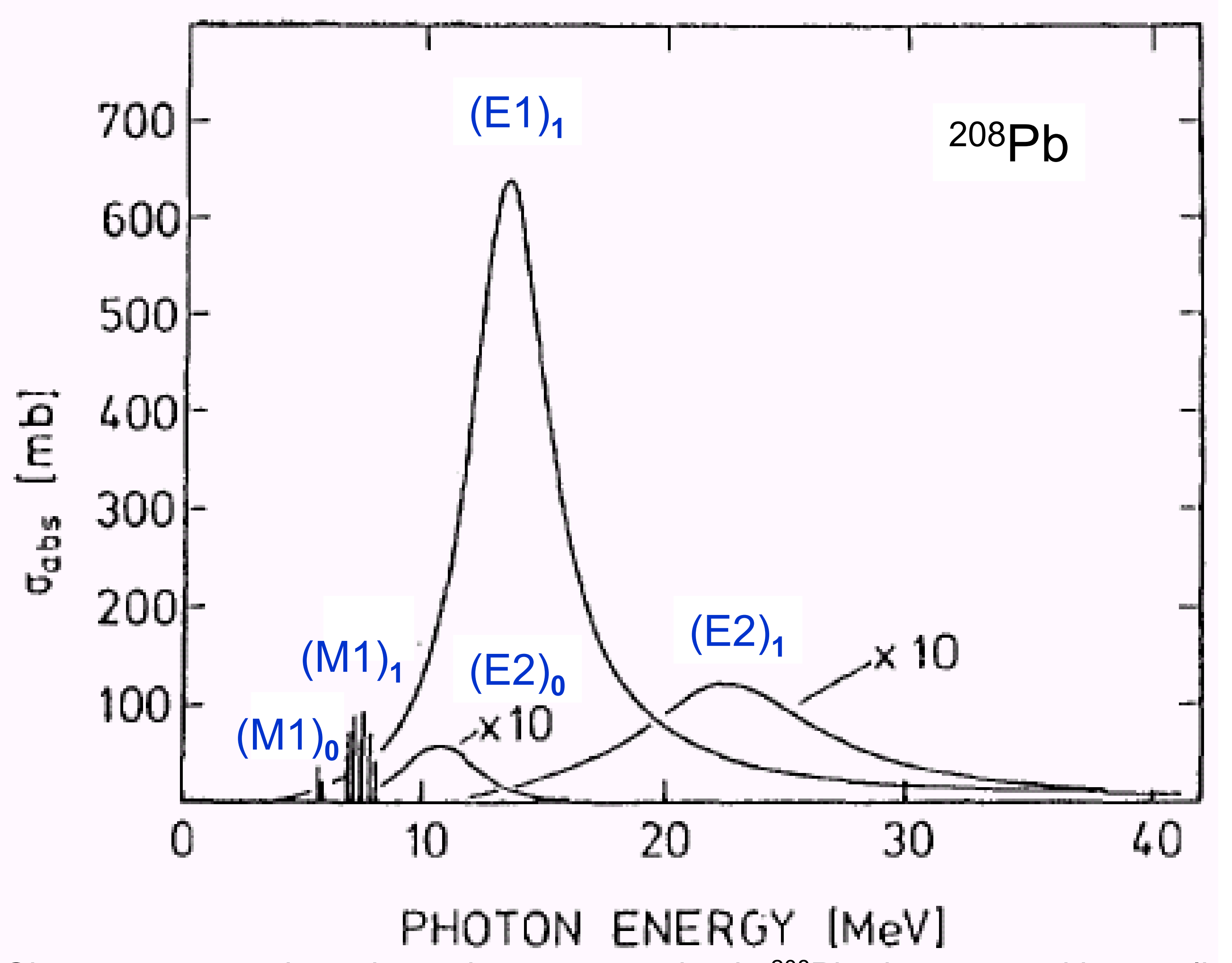

Giant resonance photoabsorption cross section in ^{208}Pb, decomposed into mulitpoles. Subscripts show isospin.

Giant Resonances

Bohr and Mottelson, vol. 2, p. 475

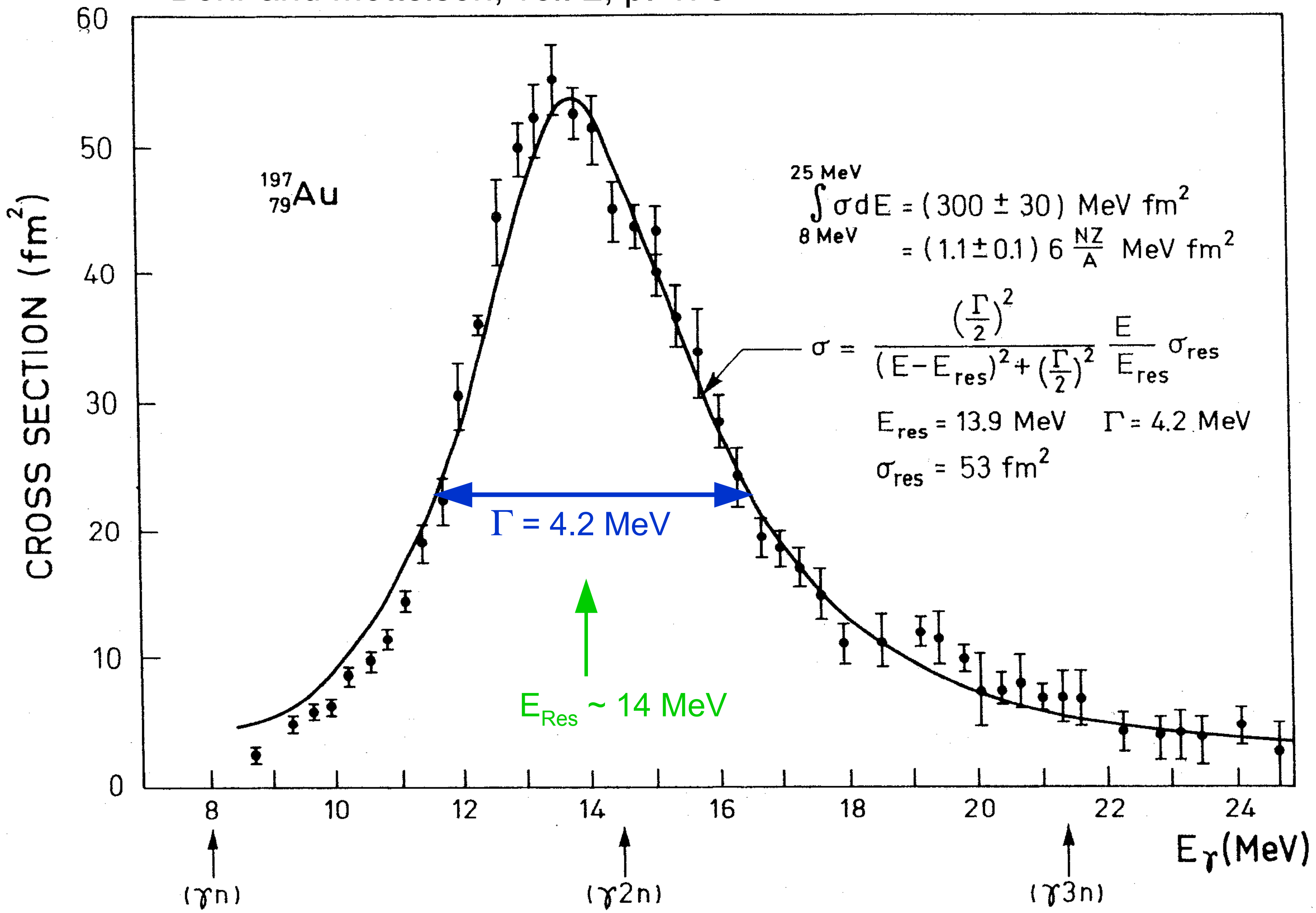

Figure 6-18 Total photoabsorption cross section for ^{197}Au. The experimental data are from S. C. Fultz, R. L. Bramblett, J. T. Caldwell, and N. A. Kerr, *Phys. Rev.* **127**, 1273 (1962). The solid curve is of Breit-Wigner shape with the indicated parameters.

In the simple geometric picture, the M1 scissors mode is the magnetic analog of the Giant Dipole Resonance.

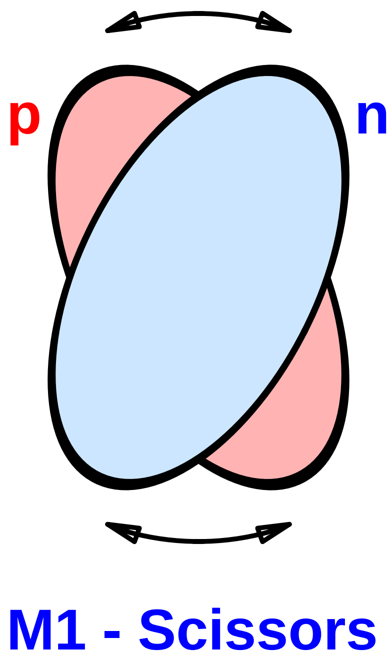

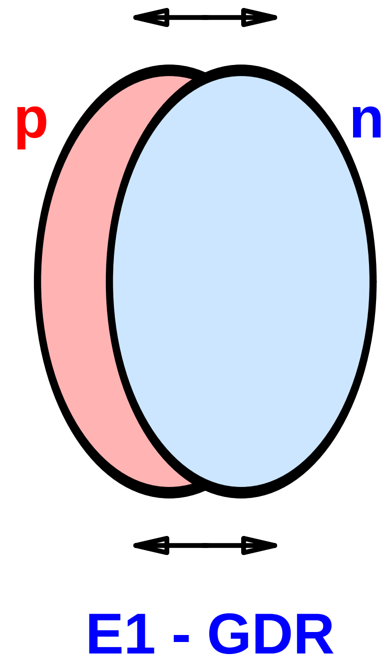

Two-Phonon GDR in ^{136}Xe

R. Schmidt et al., Phys. Rev. Lett. 70 (1993) 1767

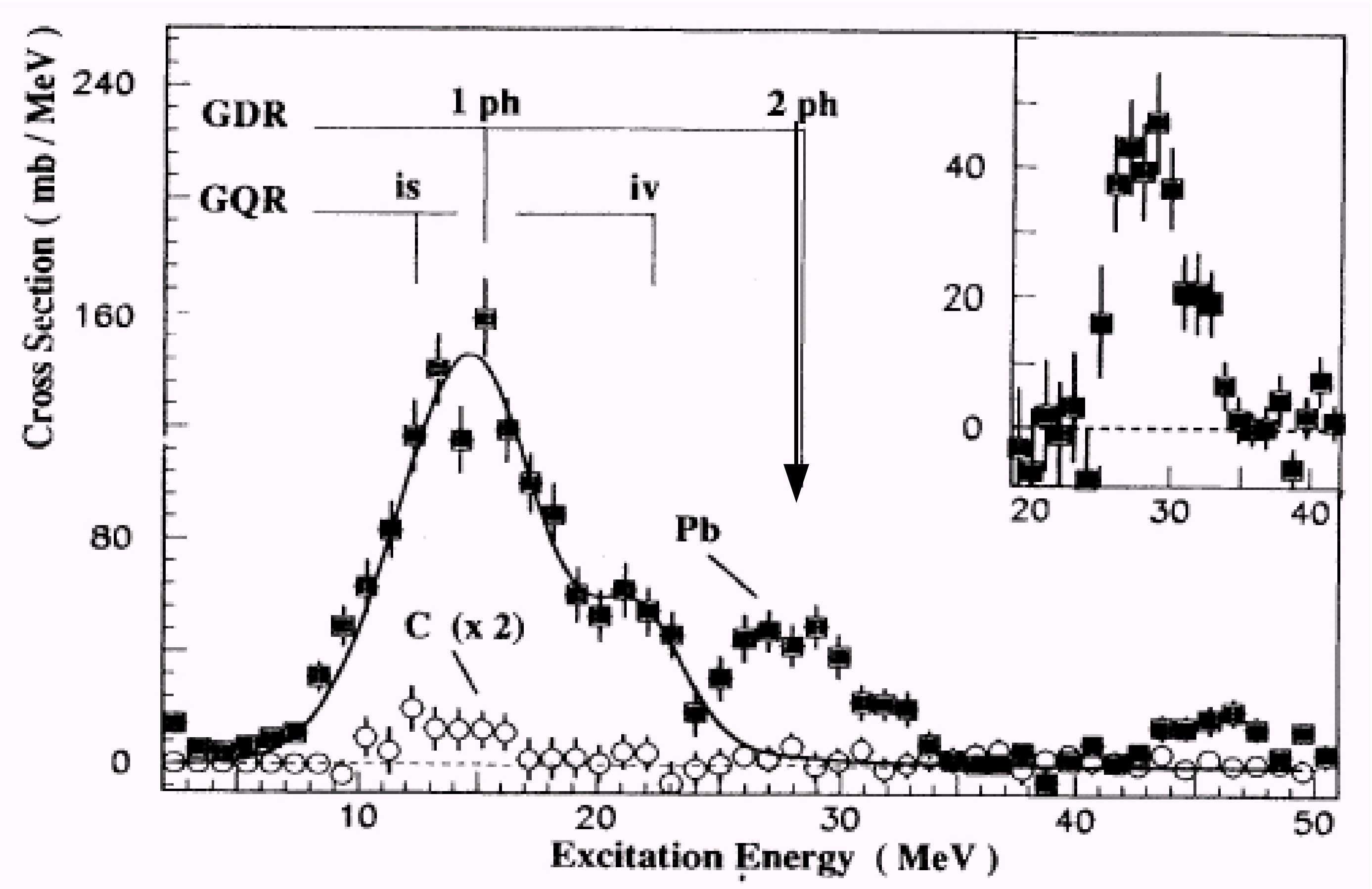

FIG. 2. Experimental results for ^{136}Xe projectile excitation on a Pb target (squares) and a C target (circles); only statistical errors are given. The spectrum for the C target is multiplied by a factor 2 for better presentation. The resonance energies for the one- and two-phonon giant dipole resonance and for the isoscalar and isovector quadrupole resonances are indicated.

Giant Dipole Resonance in Hot, Rotating Nuclei

- Populated in fusion-evaporation
- Detect GDR γ rays above tail of high-energy statistical γ rays

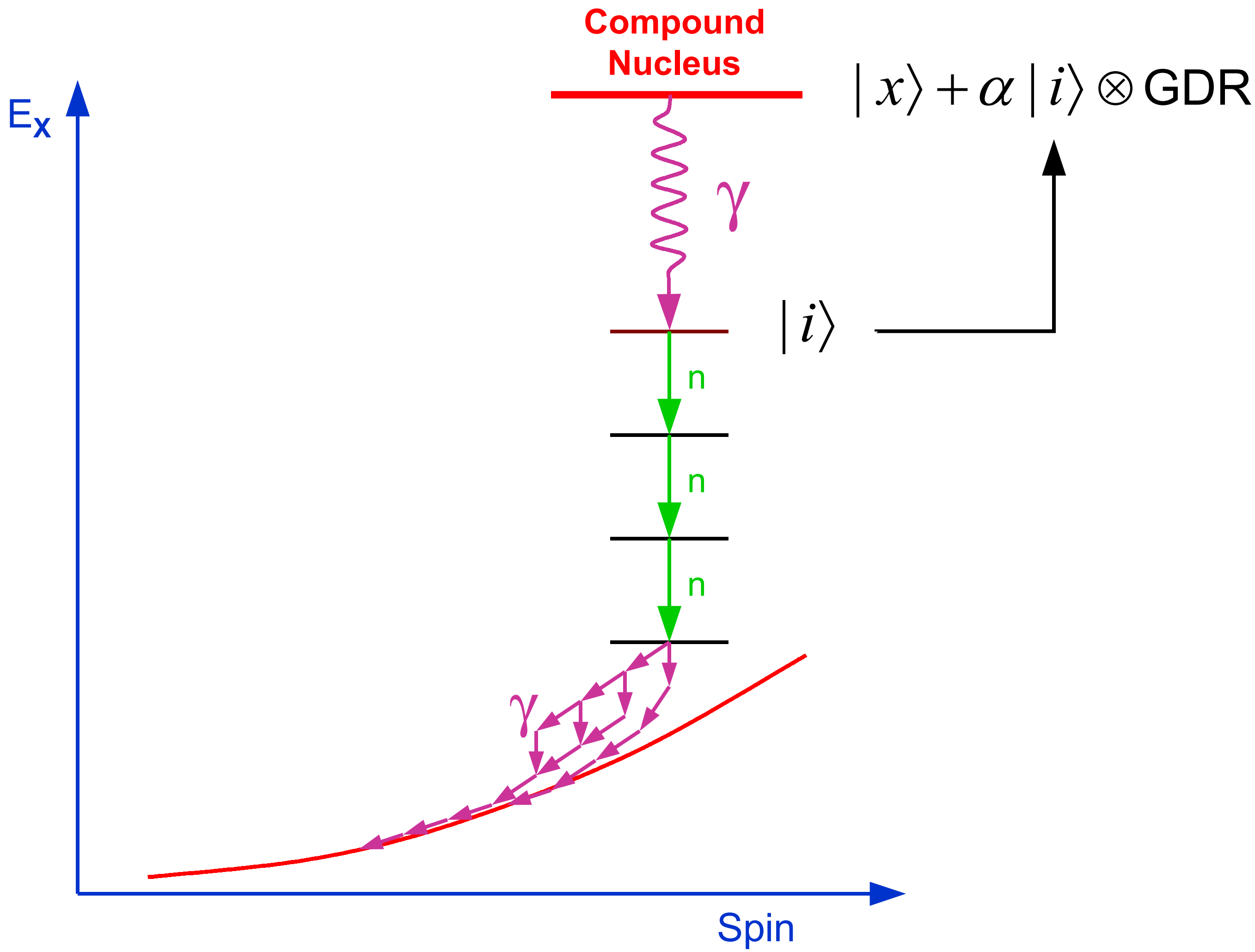

M.P. Kelley et al., Nucl. Phys. A649 (1999) 123c

$^{100}Mo + ^{18}O$; E = 125 – 217 MeV

Gammas detected in 3 large NaI detectors

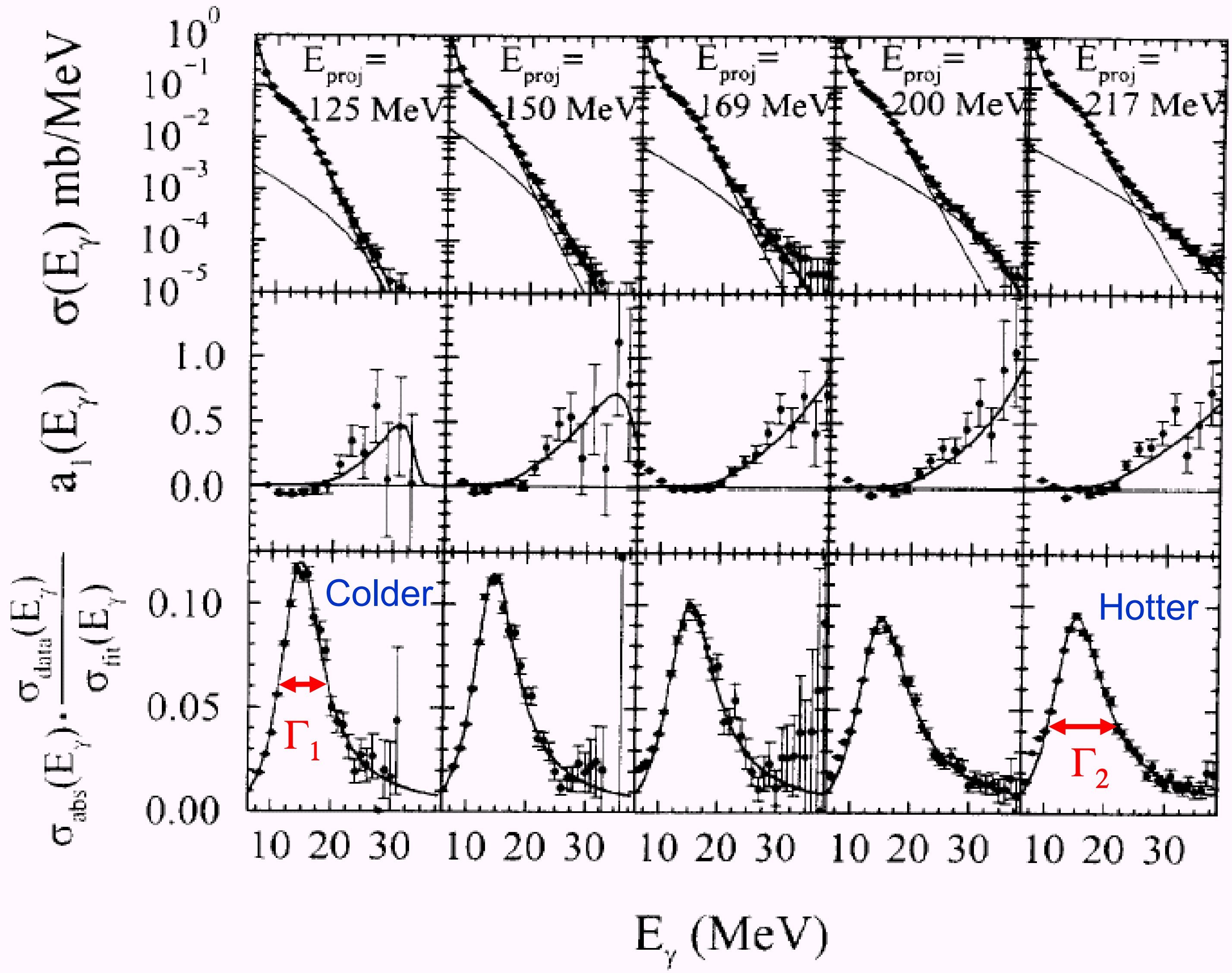

Fig. 3. Measured data and CASCADE plus bremsstrahlung fits. First row - γ-ray production cross sections. Second row - $a_1(E_\gamma)$ angular distribution coefficients. Third row - divided plots.

Y. Alhassid, Nucl. Phys. A649 (1999) 107c

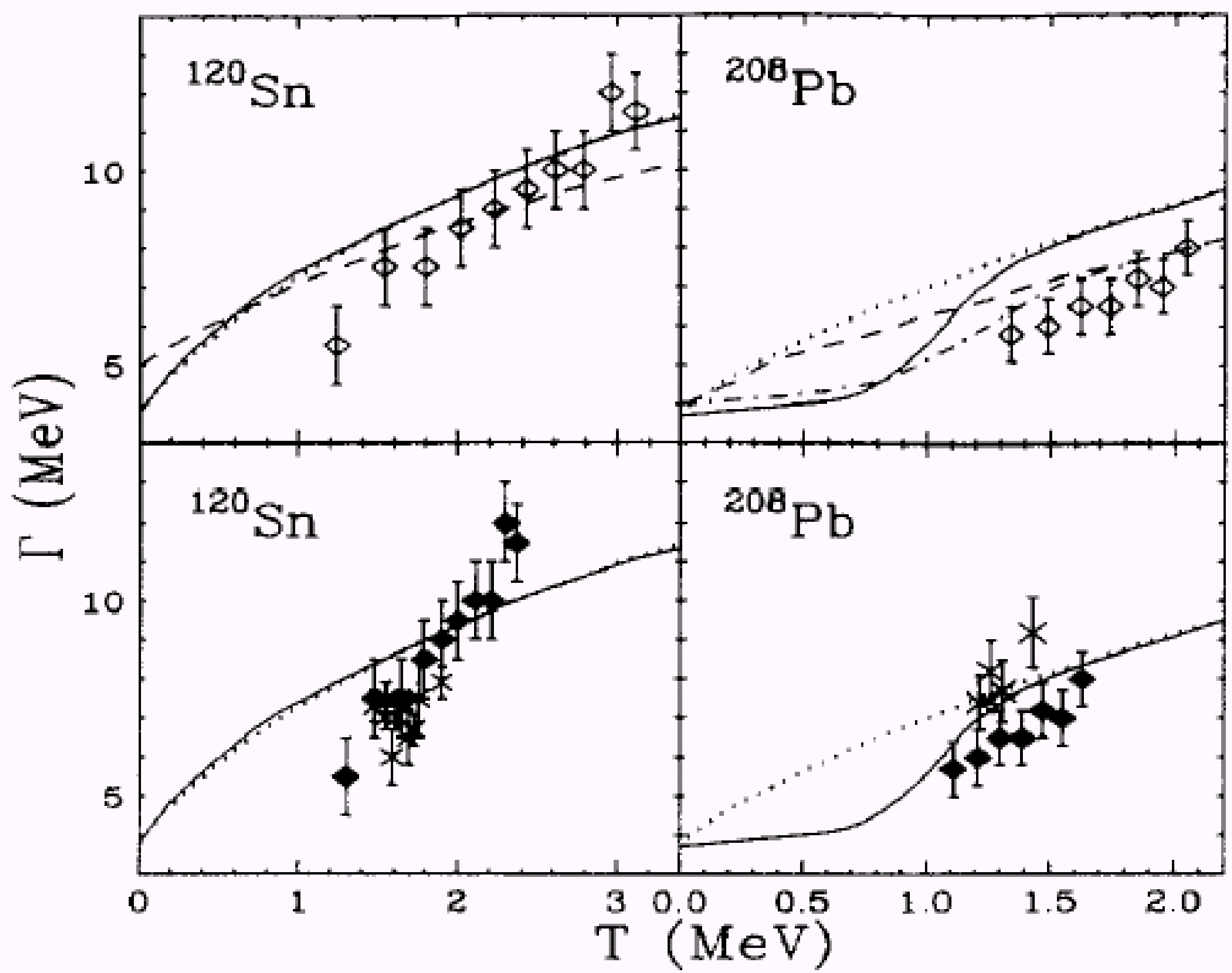

Figure 4. Temperature dependence of the GDR width in tin (left) and lead (right) isotopes. Top: the data of Refs. [16] (open diamonds) are compared to the calculations of Ref. [18] with (dash-dotted) and without (dashed) shell corrections and to our calculations [21] with (solid) and without (dotted) shell corrections. Bottom: the revised data are compared with the present calculations. The crosses are fusion data [22,19].

The Pygmy Resonance:

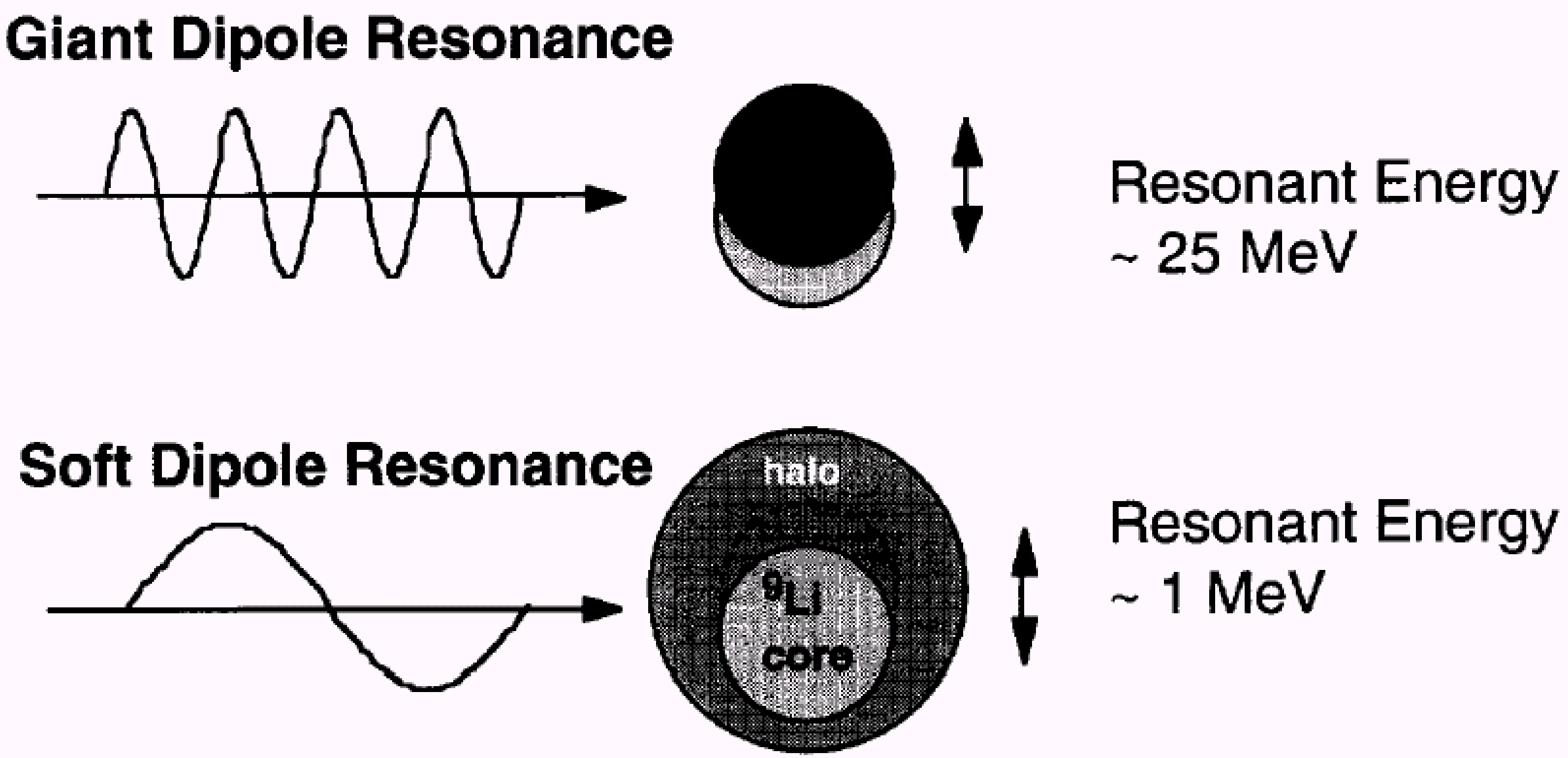

Fig. 1. Pictorial representations of the giant dipole resonance and the soft dipole resonance.

- RRPA isovector dipole strength distributions in oxygen isotopes.

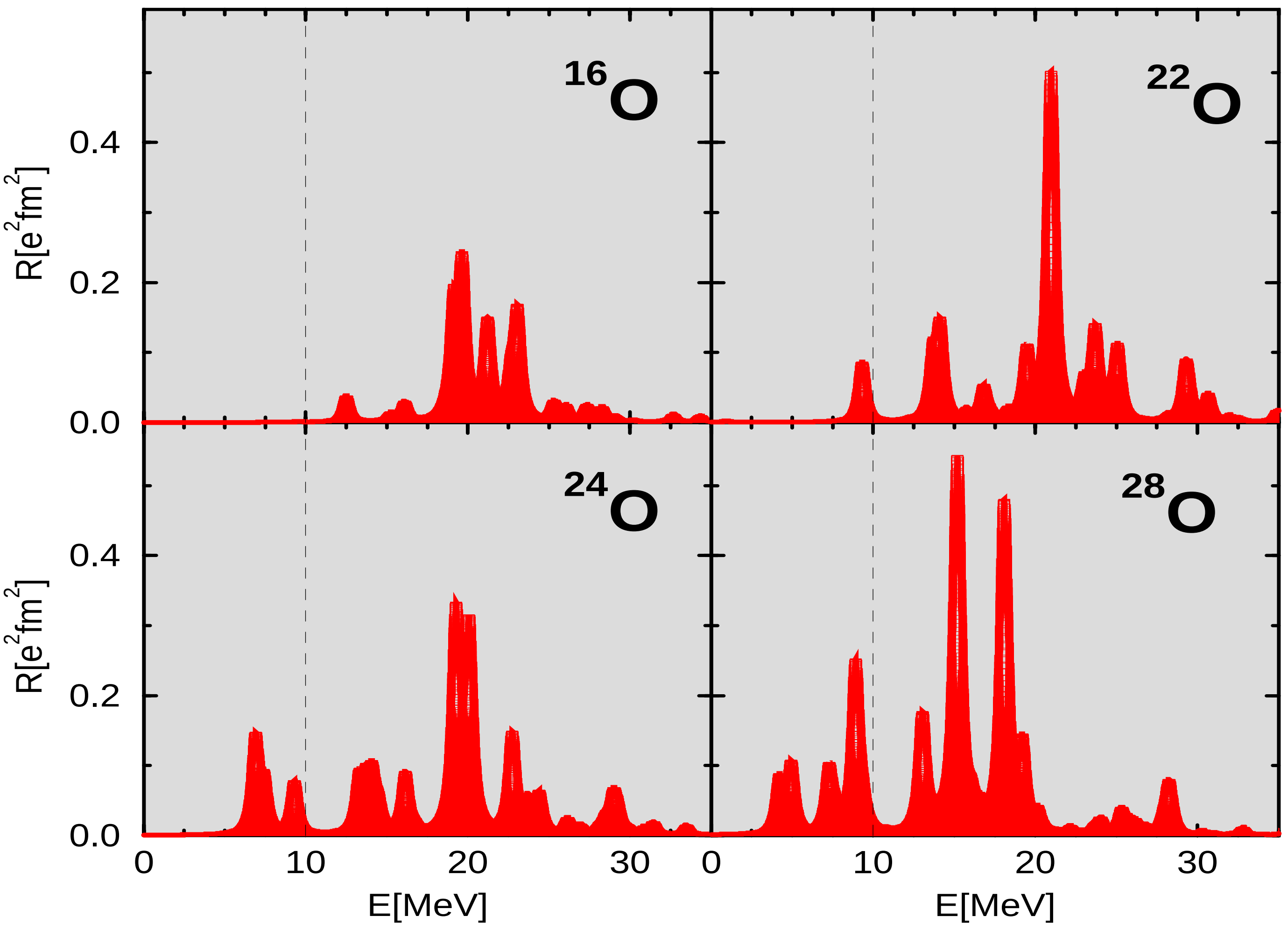

• RRPA isovector dipole strength distributions in Sn isotopes.

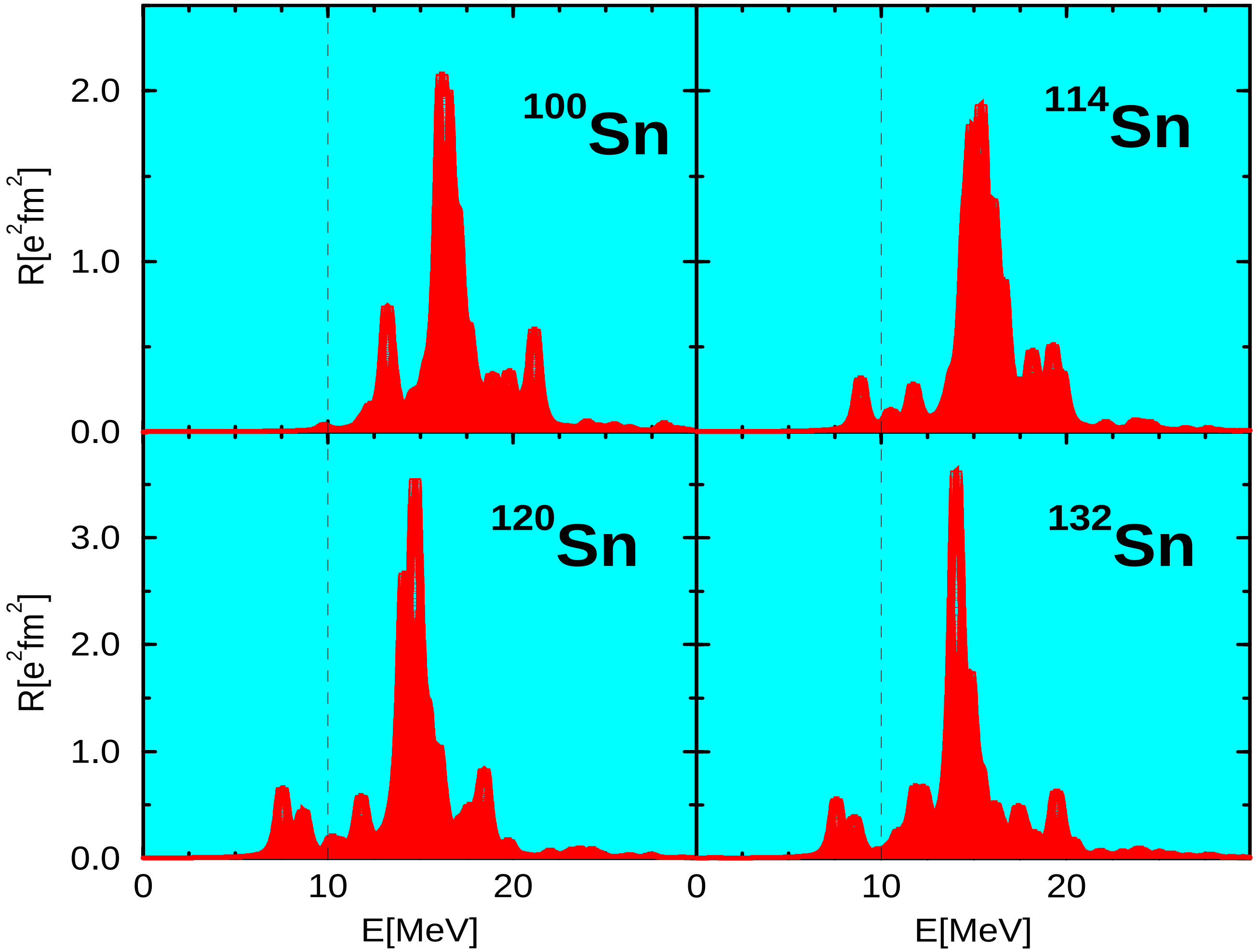

$X(\gamma,\gamma')$ - Nuclear Resonance Fluorescence

- Ideal for studying low-lying dipole collectivity

- Gamma sources: - Bremsstrahlung
  - HIGS facility at Duke University
    free electron laser

HIGS: $E\gamma$ tunable 5-8 MeV (or more?)
FWHM $\Delta E\gamma/E\gamma$ ~ 2-4%
~ 10^7 γ/s

Looking at the Target

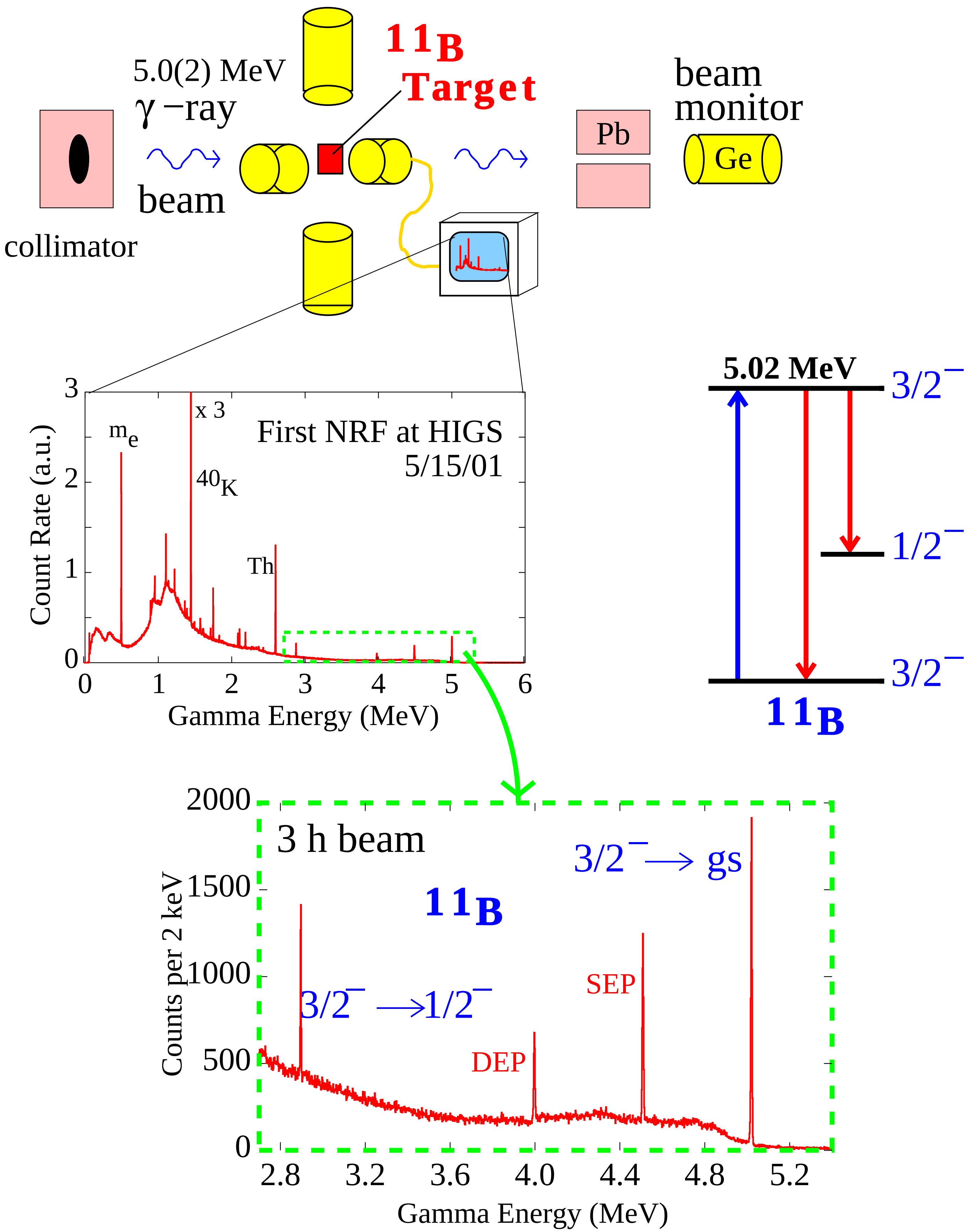

N.Pietralla et al., Nucl.Instrum.Methods A483, 556 (2002).

Parity Measurements with a Polarized Photon Beam

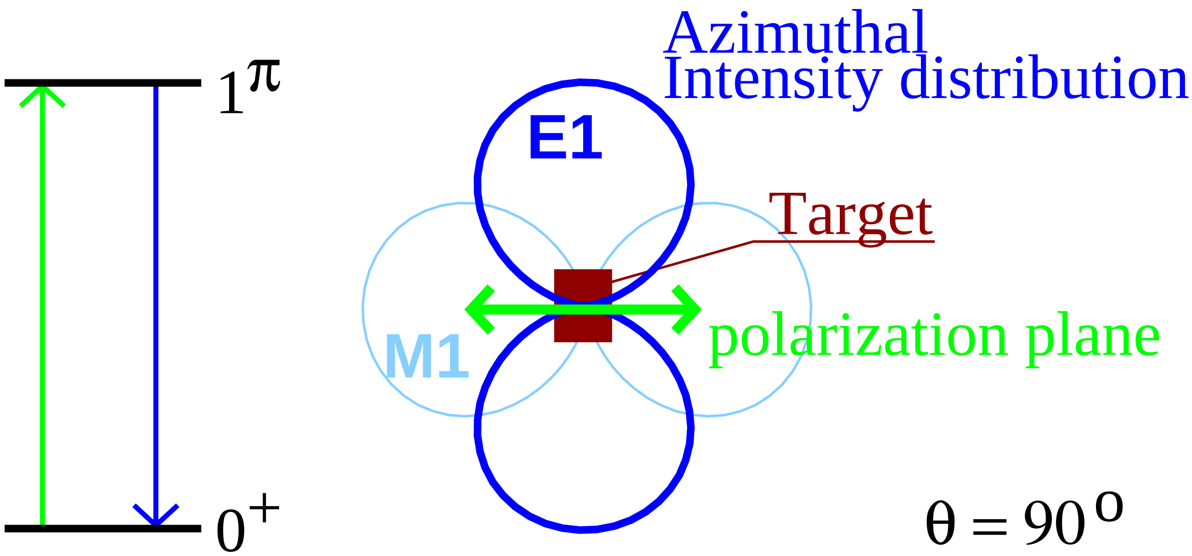

$$\Sigma = \frac{I(||) - I(\perp)}{I(||) + I(\perp)} = \begin{cases} +1 & \text{for } 1^{+} \\ -1 & \text{for } 1^{-} \end{cases}$$

TUNL/HIGS polarimeter:

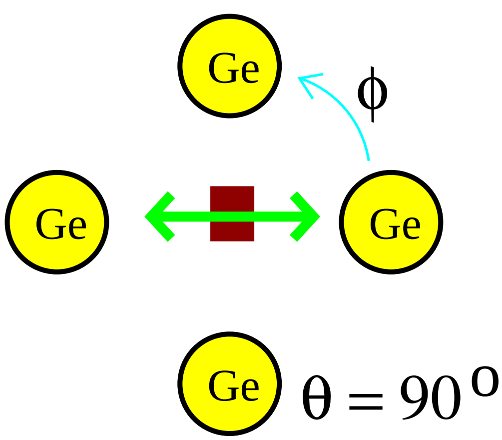

Proof−of−Principle

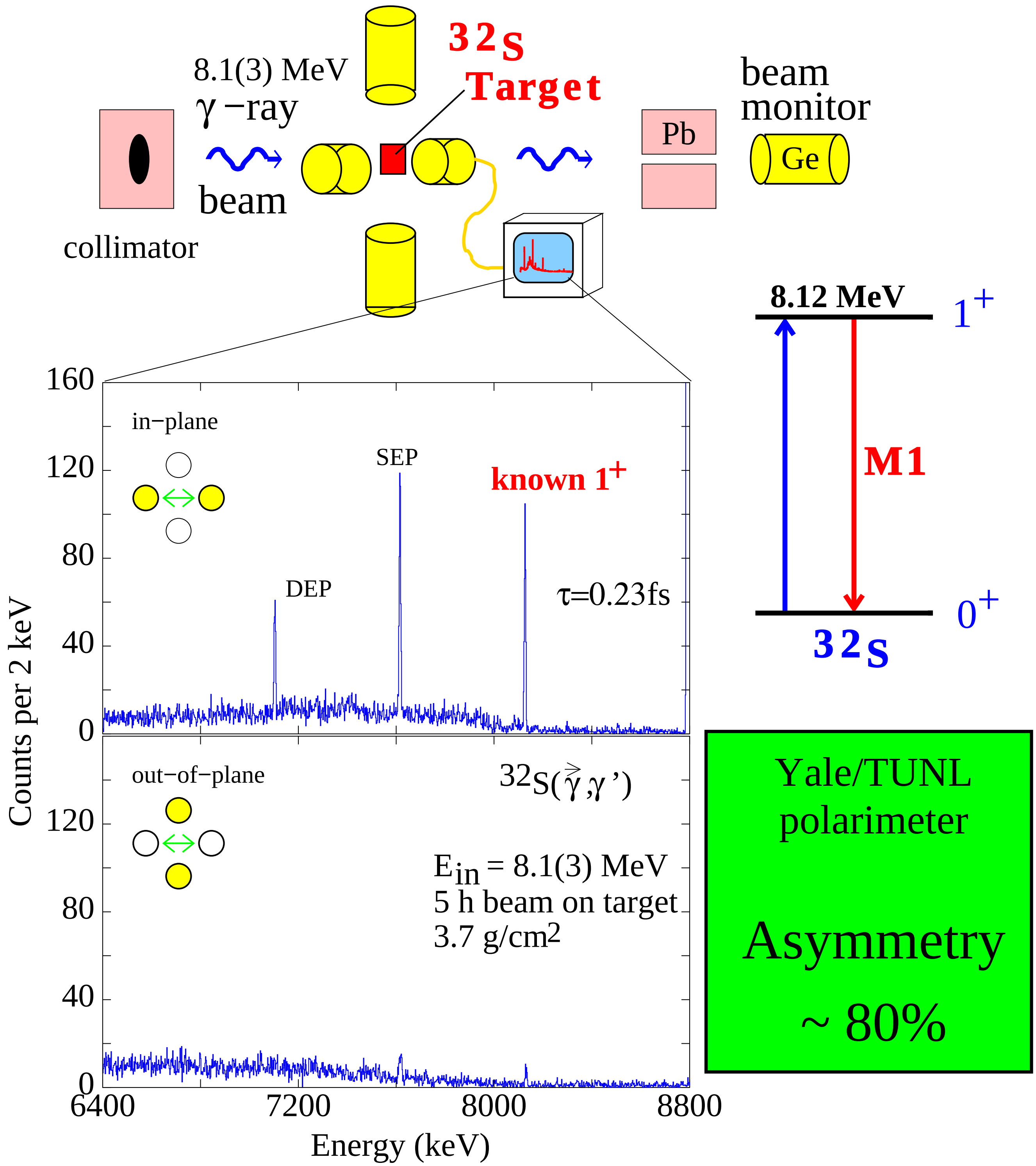

N.Pietralla et al., Nucl.Instrum.Methods A483, 556 (2002).

Polarimetry at HIgS

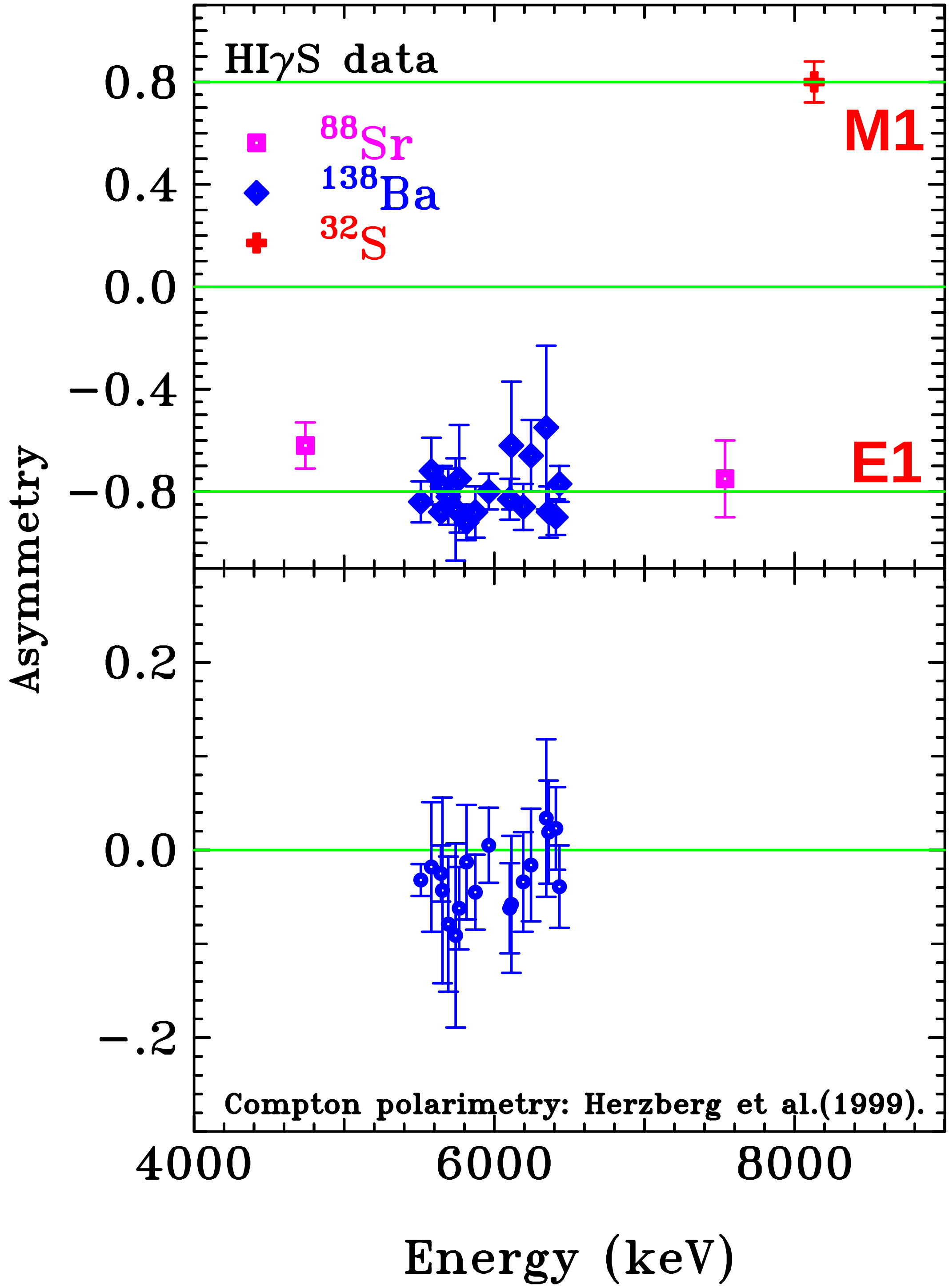

N.Pietralla et al., Phys.Rev.Lett.88, 012502 (2002).

Intermediate-Energy Coulomb Excitation

- Ideally suited for use with fragmentation beams
  $E_{Beam} \geq 30$ MeV/u

- Large cross sections ~ 100 mb
- Can use thick targets ~ 100 mg/cm^2

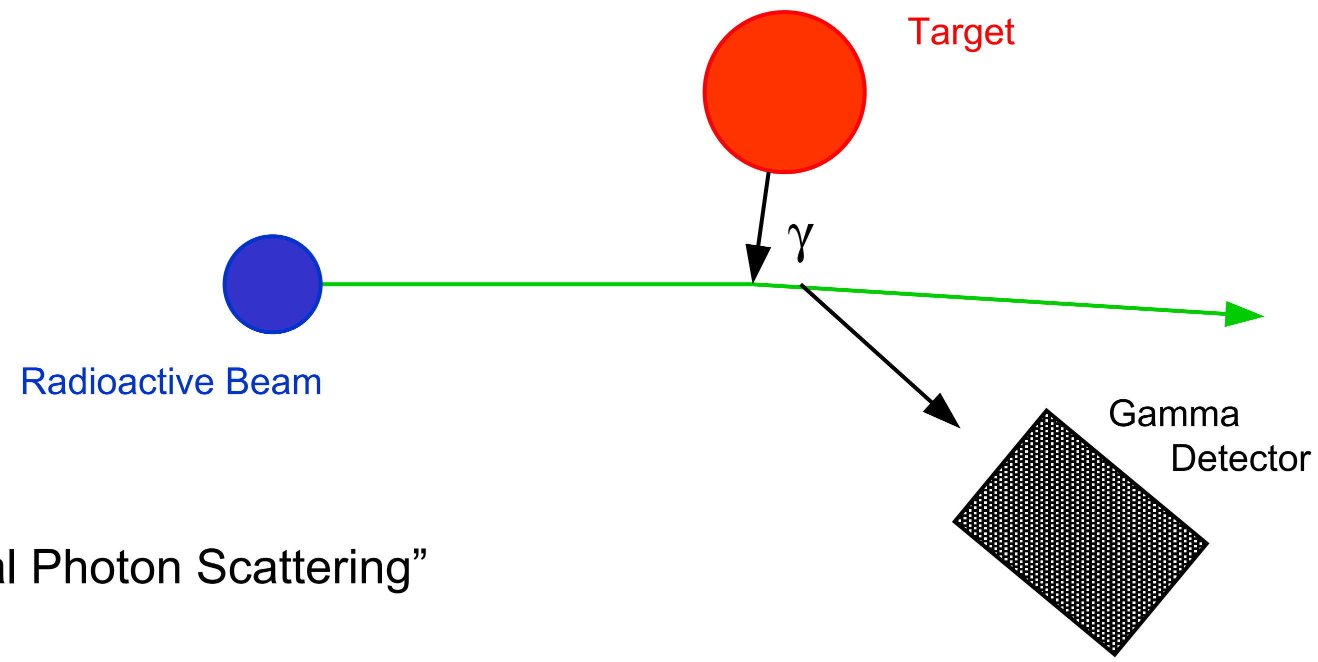

- "Virtual Photon Scattering"

Coulomb excitation in the $\pi(sd)$ shell

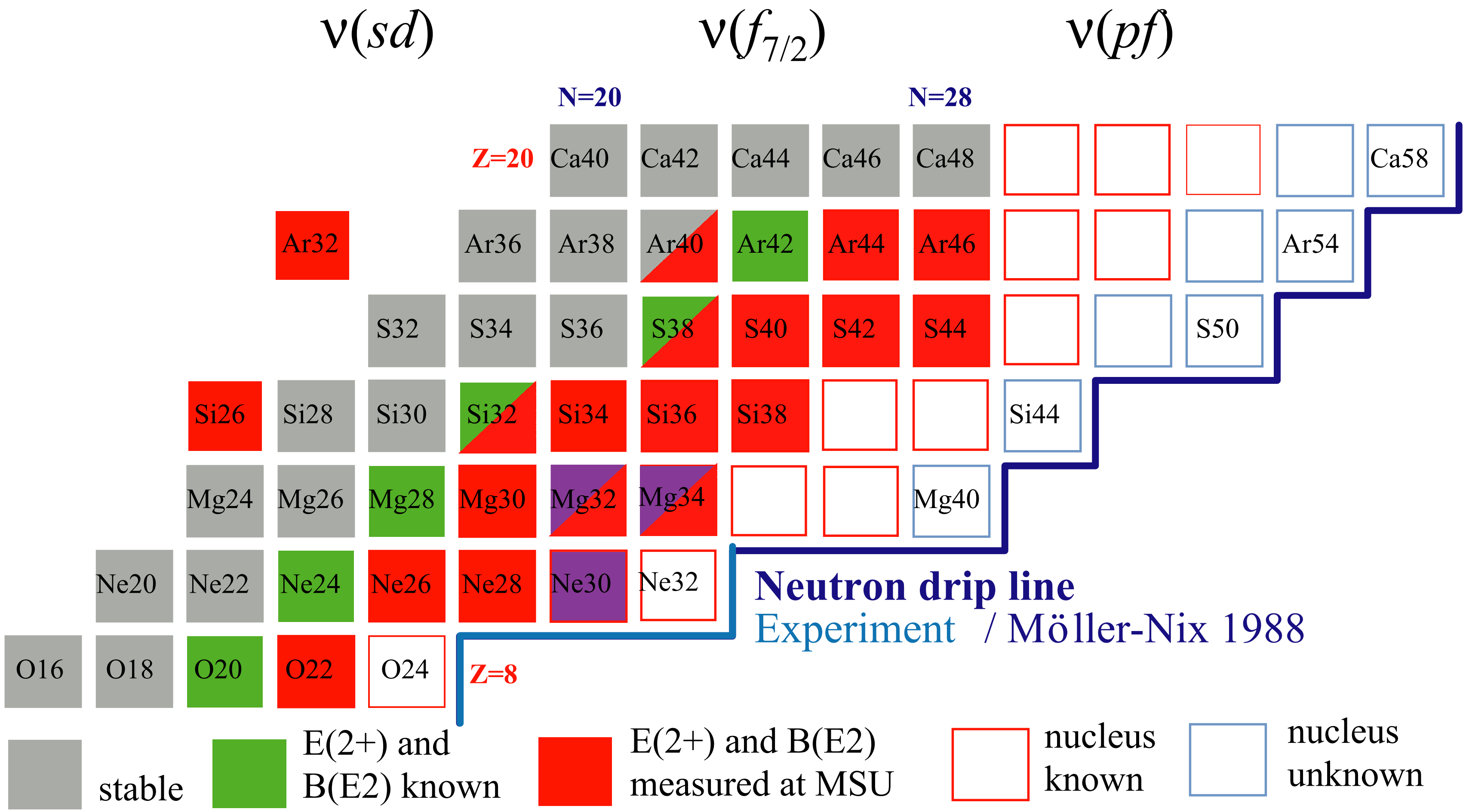

References at http://groups.nscl.msu.edu/gamma

Intermediate energy Coulomb excitation

- Ideally suited for beam-fragmentation products

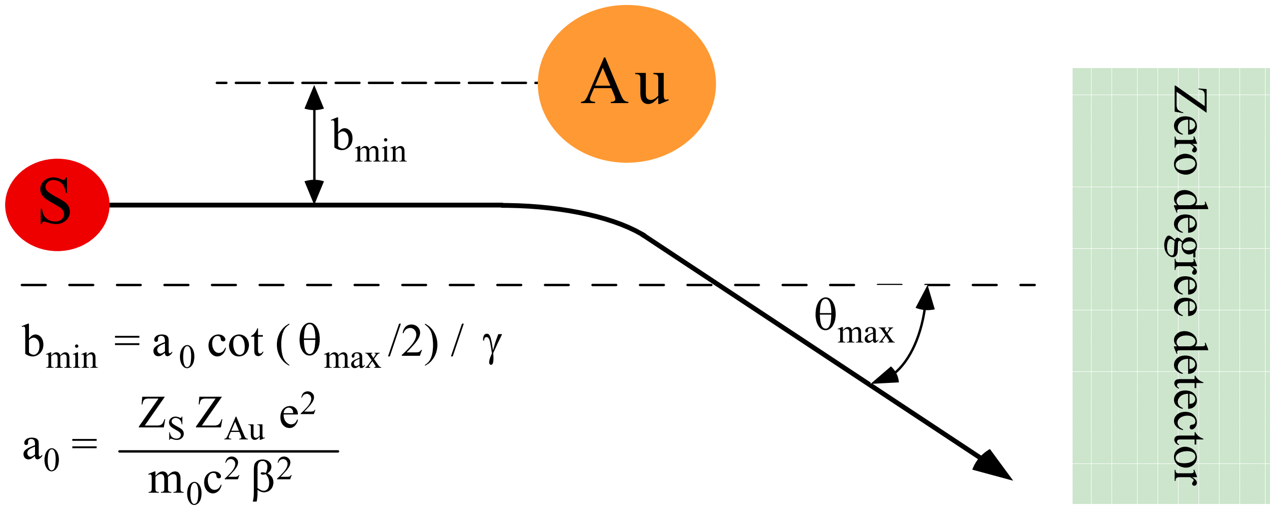

$$b_{min} = a_0 \cot(\theta_{max}/2) / \gamma$$

$$a_0 = \frac{Z_S Z_{Au} e^2}{m_0 c^2 \beta^2}$$

- $E_{beam} \approx 40$ MeV/nucl.
- $\beta \approx 0.3, \ \gamma \approx 1.05$
- $b_{min} \approx 20$ fm
- "touching spheres" $1.2(A_S{}^{1/3}+A_{Au}{}^{1/3}) = 11$ fm
- $\sigma \sim 100$ mb
- target ~ 100 mg/cm^2

- K. Alder *et al.*, Rev. Mod. Phys. **28**, 432 (1956).
- A. Winther and K. Alder, Nucl. Phys. **A 319**, 518 (1979).
- C.A. Bertulani and G. Baur, Phys. Rep. **163**, 300 (1988).
- T. Glasmacher, Ann. Rev. Nucl. Part. Sci. **48** (1998), 1.

Energy spectra in target and projectile frames for $^{40}S+^{197}Au$

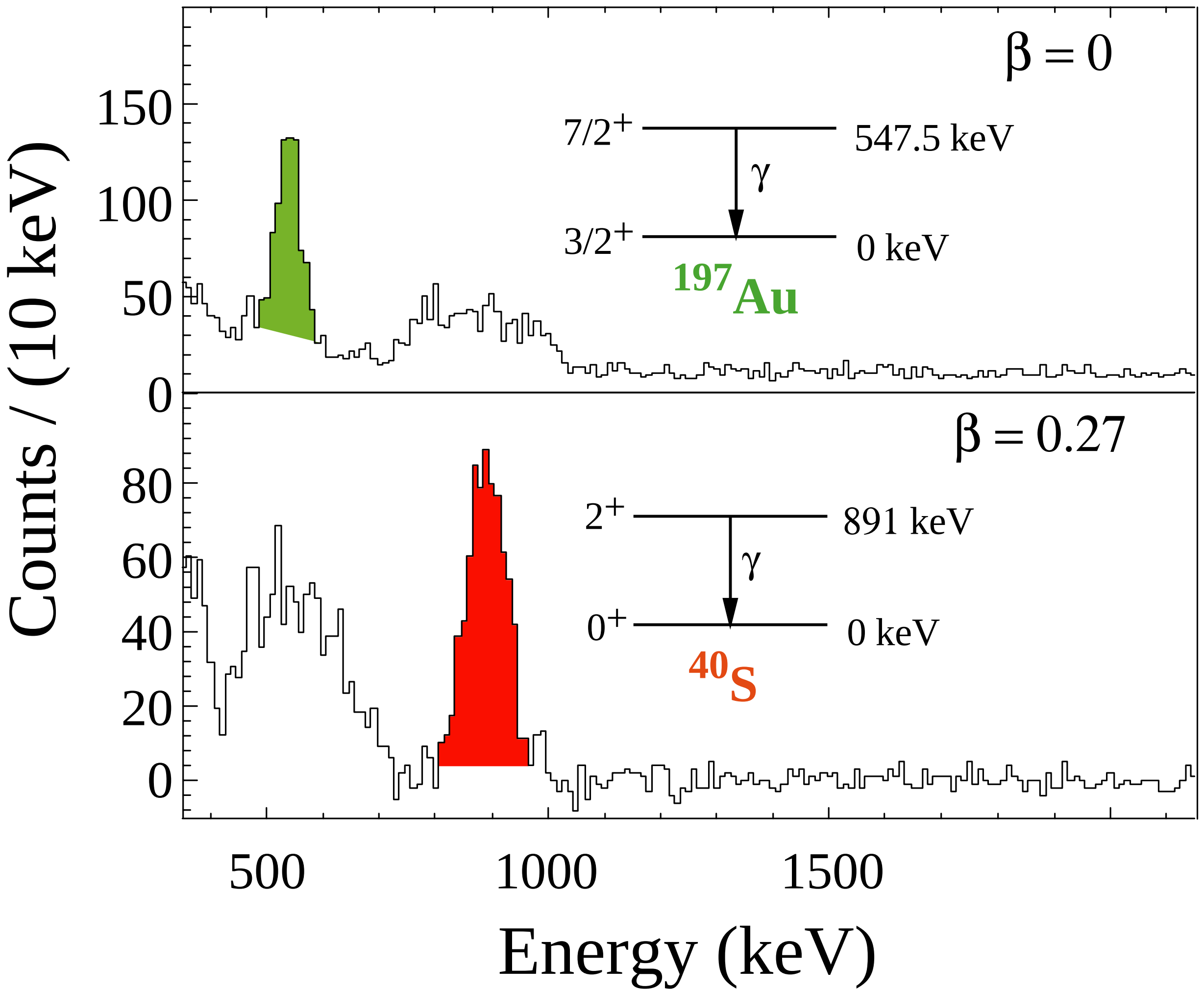

H. Scheit *et al*. Phys. Rev. Lett. **77** (1996) 3967

Deformation parameters β_2 and excitation energies $E(2^+)$: ^{30}S – ^{44}S

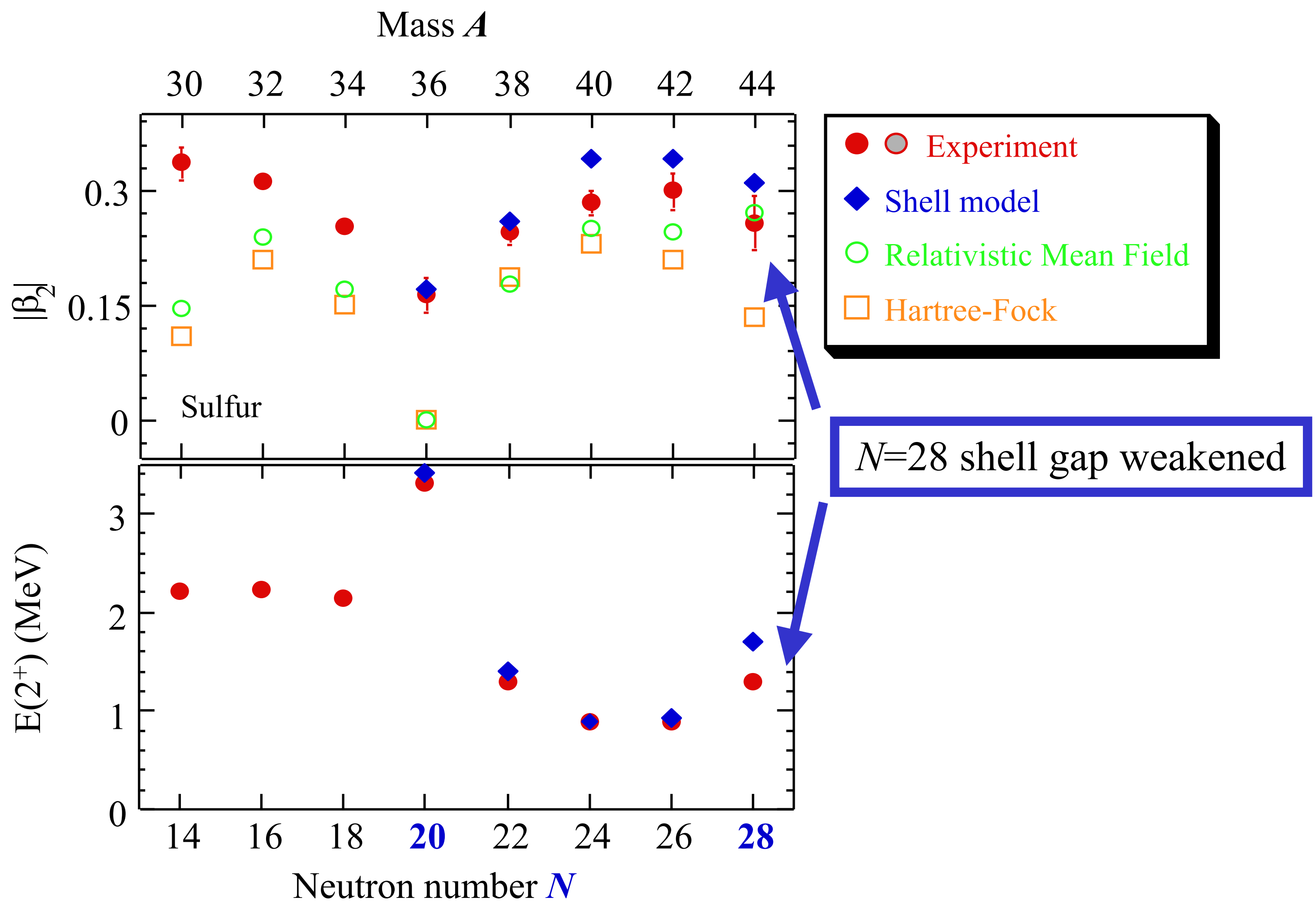

Former APEX NaI trigger barrel and Ge detectors at the NSCL

- NaI(Tl):
  - APEX trigger detector
  - 24 position-sensitive NaI(Tl) crystals
  - 20% photo-peak efficiency
  - 15% energy resolution

- Ge:
  - 18 32-fold segmented Ge detectors
  - ~0.1% - 6% photo-peak efficiency
  - <3 keV energy resolution

32-fold segmented germanium detector at Michigan State University

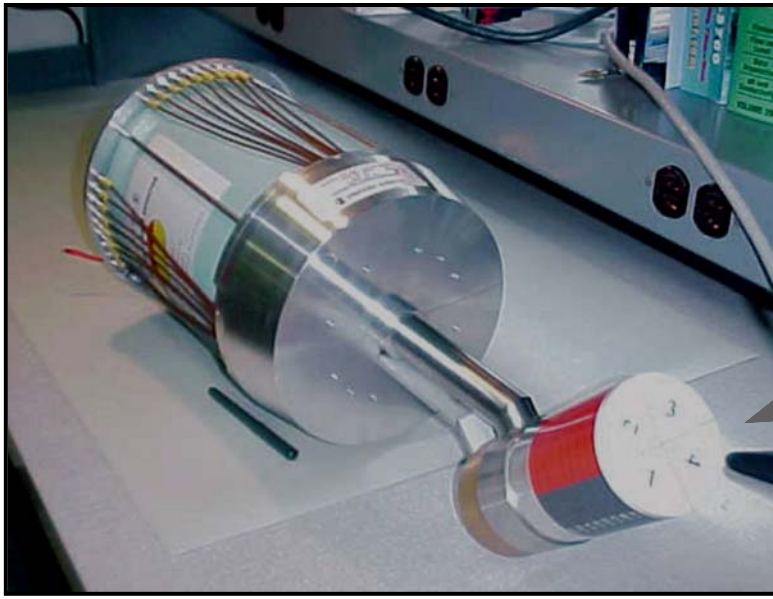

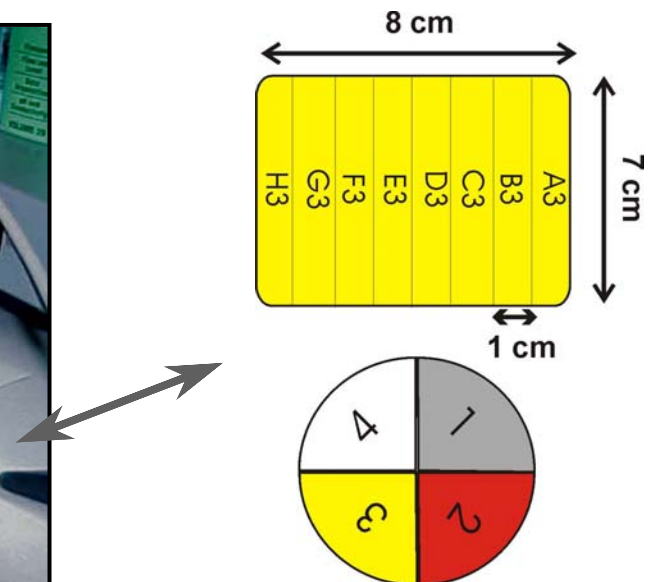

- All 18 Detectors received
  Manufactured by Eurisys Mesures
- N-type germanium crystal
  - 8 cm long, 7 cm diameter (75%)
  - 32 segments, 1 central contact, all fully instrumented with analog electronics
- Warm FETs

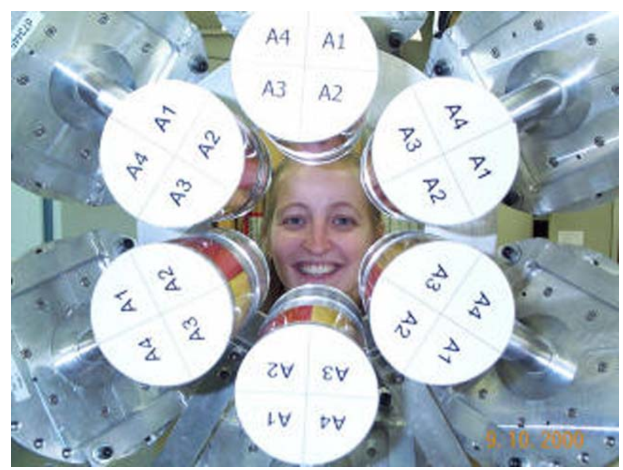

Conclusions

- A whirlwind tour of a (very) few selected topics
  in the study of collective excitations

- Great diversity!
  - There is much to be done
  - An exciting challenge: extending these
    types of studies to **RIA**